universität wien

MASTERARBEIT / MASTER'S THESIS

Titel der Masterarbeit / Title of the Master's Thesis

„Shotgun lipidomics of amnion epithelium and lung lavage“

verfasst von / submitted by

Asja Ceranic BSc

angestrebter akademischer Grad / in partial fulfilment of the requirements for the degree of

Master of Science (MSc)

Wien, 2016 / Vienna 2016

Studienkennzahl lt. Studienblatt / degree programme code as it appears on the student record sheet:	A 066 862
Studienrichtung lt. Studienblatt / degree programme as it appears on the student record sheet:	Masterstudium Chemie
Betreut von / Supervisor:	Univ.-Prof. Dr. Christopher Gerner
Mitbetreut von / Co-Supervisor:	

Abstract

Infants born prematurely suffer from immature lungs due to insufficient lung surfactant production. An essential component of the lung surfactant is dipalmitoylphosphatidylcholine (DPPC), which prevents alveoli collapse during the respiration and is therefore, important for proper lung function. Current medical lung treatments for infants use animal derived lung surfactants. The animal lung surfactant is obtained by the lavage process. Even though the lavage procedure is in accordance with the animal ethical standards, it is a quite painful process for the animals. It has been found that DPPC is also secreted by human amnion epithelium. The investigations of amnion epithelium as a DPPC source for immature lung treatment could represent a step forward, on the one hand, to reduce animal use and on the other hand to improve immunological compatibility and recycle the amniotic sack.

The aim of the study was to evaluate by lipidomic profiling whether amnion supernatant may be established as substitutes for pig lung lavage. Here we demonstrate a lipid profiling analysis by shotgun lipidomics of secreted phospholipids from amnion biopsies. Two regional sections of the amnion, which are located on the placental side and the opposite side, were separately cultivated in the DMEM and the SAGM medium. Medium fractions isolated at different cultivation times were extracted via methyl tert-butyl ether (MTBE) extraction. The profiling analysis of the MTBE extracts was performed with a shotgun lipidomics approach on a LTQ-Velos mass spectrometer. The LTQ-Velos was equipped with a TriVersa NanoMate®, Advion as a nano ion source. The lipid identification was performed via LipidXplorer software after importing the acquired negative MS/MS spectra.

We were able to optimize the shotgun lipidomics approach developed and established by Shevchenko's group and perform profiling analyzes. The obtained data demonstrated that placental amnion epithelium cultivated in DMEM as the source with the highest number of secreted lipid species. The presence of DPPC in the amnion supernatant indicates the potential to be utilized as a DPPC source. Unfortunately, two more species involved in proper lung function such as PC (16:0/14:0) and PC (16:0/16:1) have not been identified. Therefore, amnion does not yet show all desired features in order to completely replace the pig lung lavage in a lung treatment of prematurely born infants.

Zusammenfassung

Zu früh geborene Säuglinge weisen eine unreife Lunge auf, aufgrund der unzureichenden Produktion des Lungensurfactants. Um eine richtige Lungenfunktion zu gewährleisten, ist Dipalmitoylphosphatidylcholin (DPPC) als die wichtigste Komponente des Lungensurfactants essenziell, um während der Atmung einen Kollaps der Alveolen zu verhindern.

Die bisher angewändeten Lungenbehandlungen bei Säuglingen verwenden einen tierischen Lungensurfactant, der durch einen Lavageprozess dem Tier entnommen wird. Obwohl die ethischen Normen während des Lavageprozesses eingehalten werden, stellt die Gewinnung des Lungensurfactans eine schmerzhafte Prozedur dar. Kurzlich erfolgte Studien ergaben, dass DPPC auch von humanem Amnionepithelgewebe sezerniert wird.

Die Untersuchung von Amnionbiopsien als eine mögliche DPPC-Quelle für die Behandlung der Lungen von Frühgeburten könnte ein Fortschritt darstellen, um einerseits auf tierische Therapeutika zu verzichten und anderseits den amniotischen Sack zu verwerten, der bisher keiner praktischen Nutzung zugeführt werden konnte.

Im Zuge dieser Masterarbeit wurde eine Lipidprofilanalyse, der aus den Amnionbiopsien ausgeschiedenen Phospholipide, durchgeführt. Zwei ortsspezifische Abschnitte des amniotischen Sacks, von der plazentalen Seite als auch von der gegenüberliegenden, wurden in DMEM und SAGM Medium getrennt kultiviert.

Die bei unterschiedlichen Zeiten isolierten Mediumfraktionen wurden mittels *methyl tert-butyl ether* (MTBE) extrahiert und folglich die Lipidprofilanalysen auf dem LTQ-Velos Massenspektrometer durchgeführt, der mit dem TriVersa NanoMate®, Advion als Nano-Ionenquelle ausgestattet war. Die Identifizierung der Lipide erfolgte aufgrund der, in der MFQL Sprache geschriebenen Interpretationsabfragen in der LipidXplorer Software, nachdem die gemessenen negativen MS/MS Spektren in die Software importiert wurden.

Es war uns möglich die, von den Shevchenko implementierte, Shotgunmethode mit unseren Instrumenten erfolgreich zu etablieren um eine Lipidprofilanalyse durchzuführen. Die erhaltenen Daten zeigten, dass die in DMEM kultivierte plazentale Amnionbiopsie als eine Lipidquelle dienen kann, da diese die höchste Zahl an unterschiedlichen Lipidspezies aufwies. Deshalb könnte das Amnion als eine potenzielle DPPC-Quelle eingesetzt werden. Zwei weitere Spezies, die für die richtige Lungenfunktion beteiligt sind, wie PC (16: 0/14: 0) und PC (16: 0/16: 1) konnten nicht identifiziert werden. Das Amnion zeigt in der bisher hergestellten Form aufgrund dessen noch nicht das erwünschte Potential, um vollständig die Schweinelungenlavage in der Lungenbehandlung von Frühgeborenen zu ersetzen.

Acknowledgments

I would like to thank Univ. Prof. Dr. Christopher Gerner and Univ. Prof. Dr. Heinz Redl for the great opportunity to be a part of this study and Angela Lemke M.Sc. for providing the samples for our research.

Especially I would like to thank Rupert Mayer MSc. for supervising me and Anna Fabisikova MSc for technical support on the LTQ-Velos, Florian Prodinger B.Sc. for the data evaluation on the LipidXplorer, Mag. Denise Wolrab for the measurements on the SFC, and DI Dr. Johanna Mader, M.Phil for the introduction into sample preparation for proteomics.

Also, I would like to thank the rest of the Gerner group for their moral support.

Additionally, I would like to thank my parents for the unconditioned love and always being there for me, so as my sisters Lejla and Nejra and my beloved soul Ajdin. I would like to thank the God, the Hu who opened the doors and made all of this possible for me.

Contents

List of Abbreviations

EGF	Epidermal growth factor
TGF	Transforming growth factors
EPO	Erythropoietin
RDS	Respiratory Distress Syndrome
VILI	Ventilator-Induced Lung Injury
hAECs	human amnion epithelial cells
DPPC	Dipalmitoylphosphatidylcholine
SP-A	Surfactant protein A
SP-B	Surfactant protein B
SP-C	Surfactant protein C
SP-D	Surfactant protein D
PG	Glycerophosphatidylglycerol
PE	Glycerophosphatidylethanolamine
PI	Glycerophosphatidylinositol
PC	Glycerophosphatidylcholine
SM	Sphingomyelin
PA	Glycerophosphatidic acid
PS	Glycerophosphatidylserine
(L/S) ratio	Lecithin/sphingomyelin ratio
PSS1	Phosphatidylserine synthase 1
PSS2	Phosphatidylserine synthase 2
PIP	Phosphoinositolphosphates
$PI(4,5)P_2$	phosphatidylinositol-4,5-bisphosphate
CID	Collision-induced dissociation
HCD	higher-energy collisional dissociation
Cer	Ceramide
ESI	Electrospray ionization
MALDI	Matrix-assisted laser desorption ionization

QqQ	Triple Quadrupole
QTRAP	Quadrupole-linear ion trap mass spectrometer
TOF	Time Of Flight
MS	Mass spectrometry
MS1	One dimensional Mass Spectrometry
MS2	Two dimensional Mass Spectrometry
QqTOF	Quadrupole time of flight mass spectrometer
LESA	Liquid surface extraction analysis
LC	Liquid chromatography
LTQ	Linear Trap Quadrupole
ETD	electron transfer dissociation
MFQL	Molecular Fragmentation Query Language
MTBE	Tert-Butyl methyl ether
SFC	Supercritical fluid chromatography

1. Introduction

1.1. Introduction and aim

Since 2002, a growing interest in the field of lipidomics is observed (Holčapek, 2015). Several methodical approaches have found application considering the vast amount of species that lipids contribute. Shotgun lipidomics approach shows potential to be used for routine analysis, considering very fast mass spectrometric measurements without prior separation step.[1] The intent was to evaluate a shotgun lipidomics approach based on the Shevchenko's platform in order to perform lipidome profiling analysis.

Prematurely born infants are found to have insufficient lung surfactant, and therefore a treatment that involves respiratory support and co-administration of animal obtained lung surfactant as a common method is crucial for infant's survival. For the last two decades, the discoveries showed an essential role of the DPPC as the main lung surfactant component in order to achieve proper lung functionality, which mechanism was not still fully described.[2,3,4] DPPC is a glycerophospholipid with two saturated fatty acyl chains which consist of 16 carbon atoms. The aim of the study was to present the lipidome profile of the amnion biopsy surfactant as a suitable DPPC source with the untargeted shotgun lipidomics approach. According to the preliminary studies on the LBI Trauma, the amnion supernatant contains components which are present in the pulmonary. Therefore, we investigated and compared the lipid profiles of the pig lung lavage and the amnion supernatant.

Here we present new evidence that the surfactant of amnion biopsy can be used as DPPC source. Furthermore, we were able to adjust shotgun lipidomics approach on the LTQ-Velos mass spectrometer and perform very fast lipidome profiling analysis. For this purpose, two regional biopsy sections of the amnion are separately cultivated in the DMEM and the SAGM medium. Regional sections refer to the placenta associated side of the amniotic sack and the one located on the opposite side of the placenta. Isolated medium fractions at different times were extracted with methyl tert-butyl ether (MTBE). The MTBE extracts were directly infused into the LTQ-Velos mass spectrometer and MS/MS spectra were fast acquired. LTQ-Velos is equipped with the TriVersa NanoMate® nano ion source which enables conditions to generate a nano-electrospray and to work with very low sample volumes. The LipidXplorer software was used to perform lipid identifications and showed that in DMEM cultivated human placental amnion biopsy is the richest in lipid species and has the most abundant lipid profile. Lipidome profiling analysis in SAGM gives an indication that the amnion biopsy is better preserved and is therefore, less abundant.

1.2 Amnion

The Amnion is an inner embryonic membrane that covers the embryo. Although it is not part of the actual embryo it is crucial for its growth and survival. The amniotic sack is formed when the amniotic membrane expands extracting a specific fluid from the inner side of the embryonic membrane. Amniotic fluid components originate from mother's placenta and fetus secretome. Hydrostatic and osmotic forces[7] affect the fluid secretion which takes place via amnion epithelium. While 98-99% of its volume consists of water[5] it also contains components like carbohydrates, lipids, hormones, fatty acids, fetal urine, proteins, and amino acids.[6,7] Additionally, there are also growth factors, like epidermal growth factor (EGF), transforming growth factors (TGF-a and TGF-b1), insulin-like growth factor 1 (IGF-I) and erythropoietin (EPO) present in the amniotic fluid that protect and facilitate the growth of the fetus.[7]
In our experiments, we used cultivated amnion biopsies from two distinct regions, such as the placenta associated area and the reflected area (opposite of placenta) to determine the composition of the secreted lipids (amnion biopsy supernatant lipids) (see **Figure 1**).

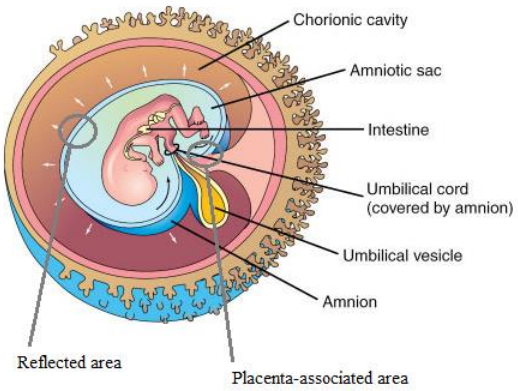

Figure 1. Extraembryonic membranes in human utero: amnion, yolk sac, allantois, and chorion. Two distinct regions of the amniotic sack are marked: the reflected area and placenta-associated area.[8]

1.3. Premature infants

Infants born prior to 37th gestation week are considered as preterm born infants. Prematurely born babies often have immature lungs and suffer from transient lack of pulmonary surfactant. The pulmonary surfactant is a lipid-protein mixture which lowers the tensions in lungs while inhaling. Infants that lack the surfactant are diagnosed with respiratory distress syndrome (RDS) and have difficulties expanding lungs during the inhalation.

To compensate this defect, treatments involving ventilators for respiratory support as well as co-administration of animal-derived surfactant directly into the lungs are required.
Infants have commonly 100 mg surfactant per kg body weight.[9] The disadvantage of using the ventilators in sensitive lungs of preterm infants for a long time period is the development of Ventilator-Induced Lung Injury (VILI). Ventilator injured lungs can be treated with stem cells like human amnion epithelial cells (hAECs), which have anti-inflammatory effects and regenerate the injured lungs.[10]

1.3.1 Pulmonary surfactant

Considering that prematurely born babies have difficulties breathing due to slow lung surfactant metabolism,[11] the determination of phospholipid composition in the amnion biopsy surfactant would be essential to develop a treatment for immature lungs.
Lung surfactant is a mixture of lipids and proteins which consist mainly of phospholipids. Dipalmitoylphosphatidylcholine (DPPC), which plays a crucial role in respiration, is found in high concentrations.[2] DPPC is used to reduce the surface tension at the liquid/air interface in the lungs and prevents the collapse of alveoli during expiration.[3] The lung surface tension should be between the minimum of 2 mN/m and the maximum of 20–25 mN/m.[4]
This optimum tension is achieved through the formation of a monolayer of DPPC in the alveoli with lipid adsorption promoter and enhancer surfactant proteins A (SP-A), B (SP-B), C (SP-C), and D (SP-D). The hydrophobic proteins SP-B and SP-C directly promote the DPPC adsorption, while the hydrophilic proteins SP-A and SP-D have an indirect role. They are involved in the assistance of hydrophobic surfactant proteins.[2]
The transport mechanism of pulmonary surfactant from type II cells to the air/liquid interface is showed in **Figure 2**.[4] As demonstrated in **Figure 2**, there are three ways of the lamellar body (LB) transport from type II cells to the air/liquid interface. In this type of transport, LBs carry the necessary surface active components (surfactant). Lamellar bodies are first built in type II cells and afterwards secreted into the lamellar subphase, located in the water medium between the type II cells and the interfacial surfactant film.
In the first transport way, there is a direct adsorption of the lamellar body at the interface including surfactant transfer. In the subphase, LBs can also unroll and build an intermediate tubular myelin (TM) or a large surfactant membrane layer. Both can be attached to the interface (second transport way). In the third transport way, surfactant membrane can be formed from lamellar bodies (surfactant surface phase) allowing the transport of surfactant to the interface.[4]

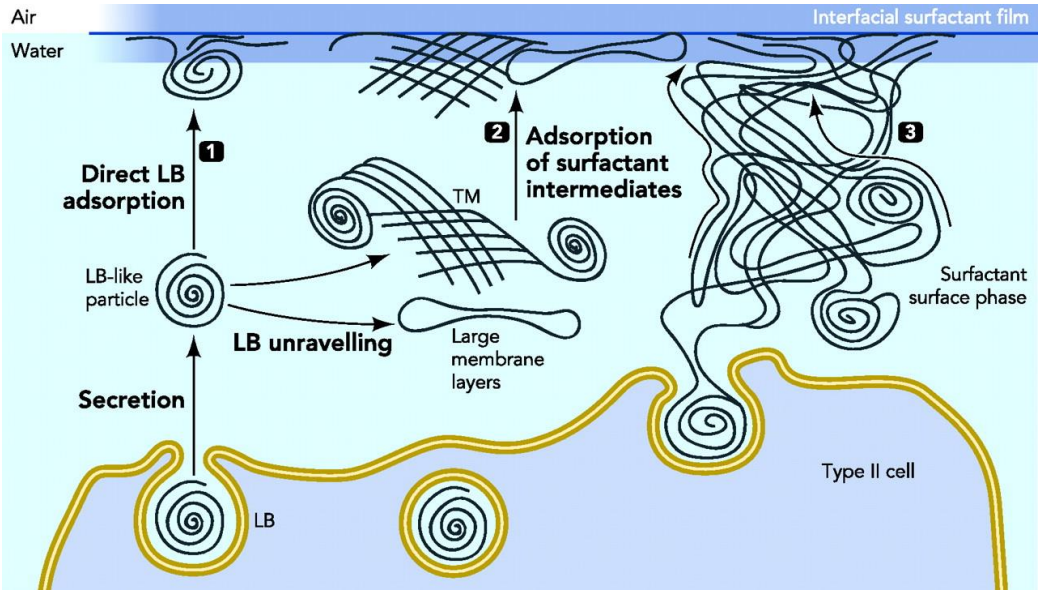

Figure 2. *The formation processes of an interfacial surfactant film. Three ways of adsorption on the air/liquid interface: (1) direct adsorption of lamellar bodies (LM), (2) adsorption of surfactant intermediates tubular myelin (TM) and large membrane layers, (3) formation of surfactant membrane. (With friendly permission of Jesús Perez-Gil)*[4]

1.3.2 Interfacial surfactant film

The pulmonary surfactant consists not just of DPPC, but also of cholesterol and unsaturated phospholipids like phosphatidylglycerols, neutral lipids and other phosphatidylcholines.[3] Pure DPPC would cause low surfactant fluidity at body temperature and slow surfactant transport from type II cells to air/liquid interface.[4] Interfacial surfactant film is generated by DPPC enrichment which takes place in two ways as described by Cockshutt.[12] Surfactant proteins A, B, C and D are important for the enhancement of the lipid adsorption into the film. In vitro studies demonstrated lowering of the surface tensions by adding SP-B and SP-C into the lipid matrix that already consisting of DPPC, PG and PA,[13] SP-B also plays an essential role in the surface film formation.[14]

1.3.3 Human Amnion Epithelial Cells

Amnion epithelial cells showed potential for injured lung treatment, and therefore can help to gain the normal function of the lungs in preterm born infants.

The introduction of Human Amnion Epithelial Cells in lung treatment can be described in two ways. First, amnion epithelial cells show the ability to be used as a source of DPPC for exogenous administration in infant's lungs, according to the preliminary studies on the LBI Trauma. This treatment is well established for animal lung surfactant as a DPPC source.[2]

Second, human amnion epithelial cells can be used as a treatment for damaged lung cells by infants which suffer from respiratory support injured lungs (VILI), considering recently investigated anti-inflammatory effects and repair capabilities of hAECs on injured lungs.[9] The reason for such behavior is that they act like stem cells and show potential to differentiate into different cell types like neuronal, bone, liver and lung cells, allowing the renewal of injured tissues after an in vivo treatment.[15]

To prove the effects of hAECs on lung inflammation, performed were animal experiments that showed promising results. Preterm born animals treated with hAECs showed: a reduced potential for abnormal lung development due to inflammation processes,[16] mitigation with hyperoxia-induced lung inflammation in neonatal mice[17] and significant reduction of the inflammation factor (IL-6) with bleomycin-induced lung inflammation in mice[18]. All mentioned experiments are based on intravenous or intraperitoneal hAECs administration.

1.4. Lipidomics

Lipids have different roles and functions in cells, some of them build up cellular membranes as their major constituents, and others are involved in cellular physiology as signaling molecules. They are also used as energy storage in the form of fat depots. The lipidome is referred to as the complete lipid profile of an organism, involved in a huge number of pathways in a biological system. These pathways are represented as a network of interactions between different lipid compounds. The lipidome was first mentioned 2001 in the scientific work of Kishimoto.[19]
Lipidomics is a study field, which covers all functional and structural information of lipids in biological systems and their interactions. The importance of lipids, as shown in genetic studies, can be demonstrated in diseases, in which the metabolism of lipids and enzymes is disrupted. This makes lipidomics alongside with nucleic acids, sugars and amino acids a subset of the larger metabolome.

In recent years, a number of published studies have shown a growing interest in lipidomics. In 2002 only two lipidomics related scientific works have been published, but in 2014 the number of publications reached 400.[20]

1.5 Glycerophospholipids (GPL)

Lipids are a structurally heterogenic compound group sharing two common properties: hydrophobicity and solubility in organic solvents, which makes the lipid classification more difficult. The LIPID MAPS lipidomics gateway developed a classification system based on biological properties for all naturally occurring lipids.[21] Glycerophospholipids belong to one of the eight major categories according to the LIPID MAPS classification system. All eight categories are shown in **Figure 3**.

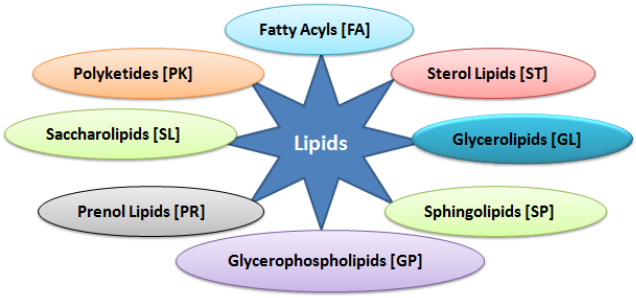

Figure 3. *LIPID MAPS lipid classification system*

As amphiphilic compounds, all glycerophospholipids structurally consist of one glycerol, esterified with two hydrophobic fatty acids and a phosphoric acid, to which one specific hydrophilic head group is bound. Considering different polar headgroups, glycerophospholipids are divided into different subclasses: phosphatidic acid (PA), phosphatidylcholine (PC), phosphatidylserine (PS), phosphatidylethanolamine (PE) and phosphatidylinositol (PI). The polar head group in PA consists only of phosphoric acid, and in other subclasses, additionally choline (as in PC), serine (in PS), ethanolamine (in PE) or inositol (in PI) are attached.

Glycerophospholipids also naturally occur as so-called “lyso” forms with glycerol esterified with only one fatty acid. For instance, lysophosphatidylcholine (LPC) is phosphatidylcholine with only one hydrophobic fatty acid remaining on the glycerol.

Another structural variation of this category is ether glycerophospholipids termed “plasmalogens”, including one or two hydrophobic carbon chains bonded to glycerol via ether instead of an ester linkage. These ether lipids are present in mammalian cellular membranes and anaerobic bacteria.

1.5.1 Biological functions of glycerophospholipids

Glycerophosphatidic acid (PA) is the simplest subclass and serves in the biological environment as a precursor for biosynthesis of other glycerophospholipids and as signaling molecule for their catabolism.[22]

Glycerophosphatidylcholines (PC) are the most abundant subclass. They commonly constitute biological membranes and pulmonary surfactant. Potential diseases by yet unborn infants can contribute to higher levels of PC in the amniotic fluid. Determination of phosphatidylcholines in the amniotic fluid and the (L/S) lecithin/sphingomyelin ratio are one of the first methods for indication of the lung immaturity.[23] The higher the (L/S) ratio in the amniotic fluid, the more surfactant is present in the lungs of infants. A value of less than 2 is an indication of the lung immaturity.[24] Phosphatidylcholines were first discovered by a French biochemist Theodore Nicolas Gobley, who isolated them from egg yolk and named them lecithins.

Glycerophosphatidylserines (PS) as constituents of biological cell membranes, are involved in cell signaling pathways, apoptosis and also play an important role in the brain. PS are mostly applied in the form of food supplements nowadays to enhance cognitive abilities and also as medicines against mental diseases such as Alzheimer's. In mammalian cells, PS is synthesized from PC or PE by headgroup exchange with two enzyme isoforms of phosphatidylserine synthases: PSS1 and PSS2.[25] Besides brain, high amounts of PS are also found in the kidneys and the testicles. PE is predominantly used as biosynthesis precursor in the brain and PC as a precursor in the kidneys and testicles.[26] Apoptotic cells tend to be removed by macrophages or other phagocytes in the tissues. This leads to cell surface changes by requisite markers of apoptotic cells, recognized by macrophages. In this case, phosphatidylserines are markers for apoptotic cells. In normal cells, they are present in the inner layer of membranes and in the apoptotic cells they are exposed on the outer membrane surface with enzyme flippase. Phosphatidylserines serve in such a way as markers for macrophage attachment.[27]

Glycerophosphatidylinositol (PI) as a membrane glycerophospholipid usually occurs in cells phosphorylated on the third, fourth and/or fifth position in the inositol ring as monophosphate, biphosphate and triphosphate. These are known as phosphoinositolphosphates or phosphoinositides (PIP). Phosphatidylinositols located on the cytosolic side of membranes are involved in intracellular signal transductions, where signaling events for different pathways take place via PI specific phosphorylation. Phosphatidylinositol-3,4,5-triphosphate (PIP3) is for instance involved in signaling pathways for cellular metabolism and regulation of gene expression.[28] The phosphorylation pattern of PI in the membranes gives also specific identity

information of cells and can act as a biomarker for cancer cells in the prostate.[29] In the plasma membrane the most abundant phosphorylation of PI is in the form of phosphatidylinositol-4,5-bisphosphate [$PI(4,5)P_2$].

Glycerophosphatidylglycerol (PG) as anionic subclass predominantly constitutes human pulmonary surfactant and biological membranes. PG plays a crucial role in the development of thylakoid membranes in chloroplasts and is therefore important for photosynthesis.[30] In the amniotic fluid, the amount of PG as well as PC, are good indicators of infant lung maturity. Glycerophospholipid contained in amniotic fluid can with 99% probability show the absence of neonatal distress syndrome by the unborn infant.[31]

1.5.2 Fragmentation of glycerophospholipids by CID

The determination and the identification of glycerophospholipids is usually performed by mass spectrometric analysis with soft ionization techniques. Depending on the applied voltage polarity in the electrospray ion source (ESI), positive $[M+H]^+$ or negative $[M-H]^-$ charged adduct ions are formed. Negative ion adducts are in general more abundant when compared to the respective positive form.[32] It is demonstrated that PS and PI in the positive ion mode additionally form sodium adducts $[M+Na]^+$.[33] In PC both protonated and sodium adducts can be formed by binding of the proton or the sodium to the phosphate group.

To achieve better electrospray ionization efficiency, it is generally more favorable, for almost all glycerophospholipids, to add a buffer in specific concentrations. Ammonium acetate and ammonium formate are common used buffers which cause the formation of acetate $[M-OAc]^-$ or formate $[M-OFor]^-$ ion adducts in the negative polarity mode. In MS spectra they can be found together with deprotonated ion adducts. Which of these adducts will be formed, depends on the glycerophospholipid subclass. Despite the presence of buffer salts, the subclasses such as PA, PS, PG and PI favor forming deprotonated adduct ions $[M-H]^-$ (LIPID MAPS online tools for lipid research). In contrary, PCs are found preferentially as acetate or formate adduct ions in the electrospray. Acetate or formate ions quench the positive charge of quaternary nitrogen in the PC so that the negative charge remains on the phosphate.[33]

Each glycerophospholipid has its characteristic fragmentation pattern and can be obtained with LIPID MAPS fragmentation prediction tool (LIPID MAPS online tools for lipid research). The only disadvantage of LIPID MAPS is the limitation to use fragment prediction just for the negative ion mode. This makes the interpretation for the positive ion mode more difficult if self-generated reference standard MS/MS spectra are not available. Collision-induced dissociation

(CID) contributes to the formation of several fragments that are characteristic for the glycerophospholipids. These fragments correspond to the neutral losses of acyl chains as fatty acids or ketenes from sn-1 or/and sn-2 positions as (see **Figures 4,5,6**).[32]

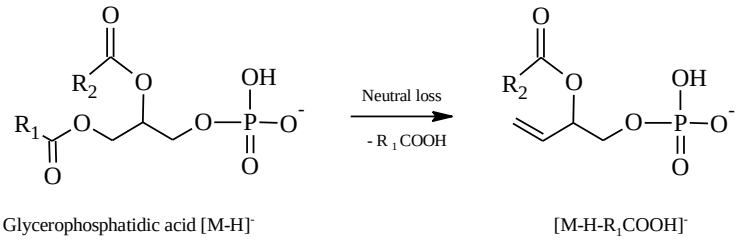

Figure 4. *Neutral loss of the acyl chain as fatty acid in sn-1 position from the glycerol phosphatidic acid as [M-H]-.*

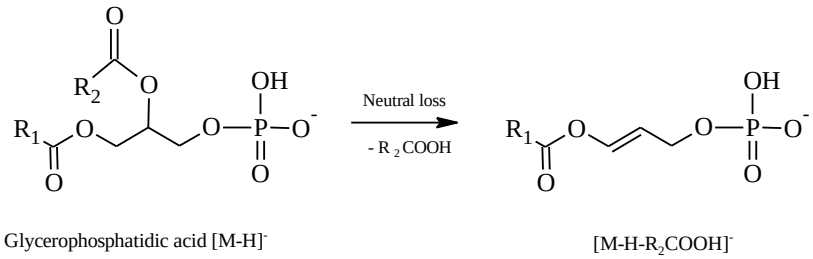

Figure 5*. Neutral loss of the acyl chain as fatty acid in sn-2 position from the glycerol phosphatidic acid as [M-H]-.*

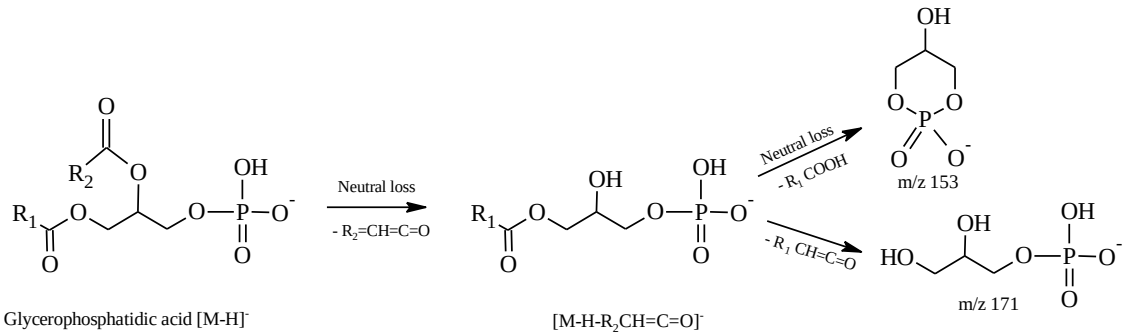

Figure 6. *Neutral loss of the acyl chain as ketene from the sn-2 position from the glycerol phosphatidic acid [M-H]-. Further, the acyl chain from sn-1 position in the [M-H-R2CH=C=O] can be cleaved as fatty acid or ketene.*

Other fragments are subclass-specific. For PC the [M-74]- fragment is characteristic, which is found as most abundant in spectra. It corresponds to the loss of the acetate and the methyl group from the quaternary nitrogen in the choline (see **Figure 7**).

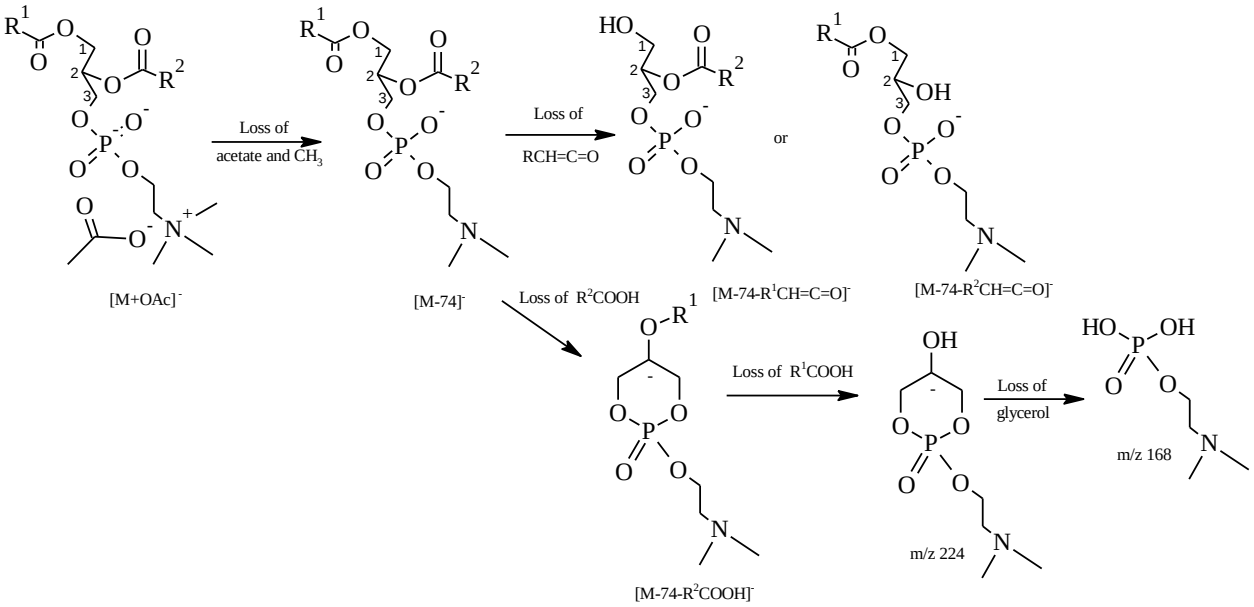

Figure 7. *The PC fragment pattern after collision induced dissociation (CID) from its precursor ion [M+OAc].*[-] [34]

The loss of inositol with the mass difference of 162 m/z is a common fragment for the whole phosphatidylinositol class. The same applies to PS and PG with the subclass characteristic loss of serine and glycerol. **Tables 1 and 2** show the typically predicted fragments for PI, PG and PS in the negative ionization mode from LIPID MAPS.

Table 1. *LIPID MAPS predicted fragments for PS and PI as [M-H]- adduct ion in the negative ionization mode*

Phosphatidyserine (PS)

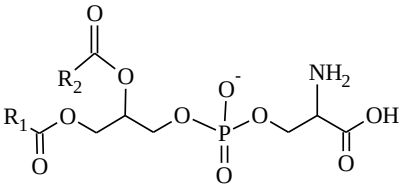

Phosphatidylserinne [M-H]-

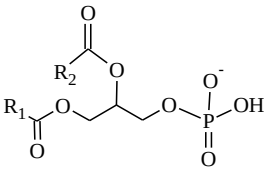

Loss of serine from [M-H]-

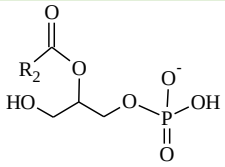

Loss of acyl chain as ketene from sn1

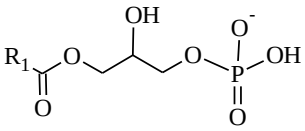

Loss of acyl chain as ketene from sn2

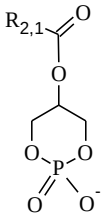

Neutral loss of RCOOH from sn1 or sn2

RCOO-

Fatty acids

Phosphatidylinositol (PI)

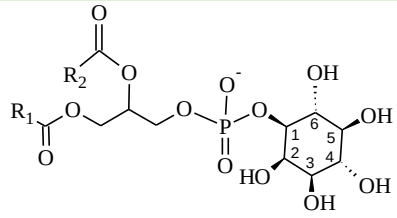

Phosphatidylinositol [M-H]-

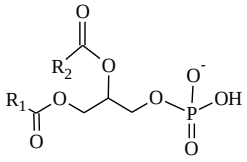

Loss of inositol from [M-H]-

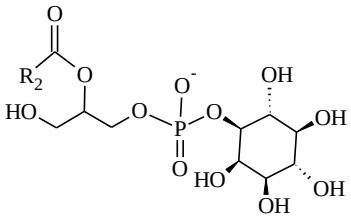

Loss of acyl chain as ketene from sn1

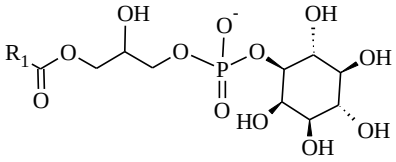

Loss of acyl chain as ketene from sn2

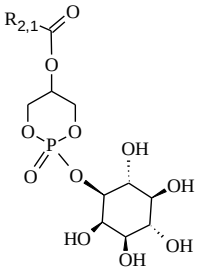

Neutral loss of RCOOH from sn1 or sn2

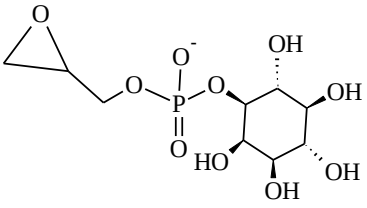

Glycerophosphoinositol -H_2O (m/z 315)

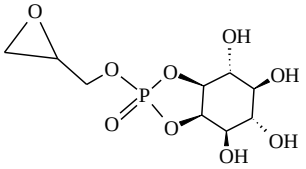

Glycerophosphoinositol -$2H_2O$ (m/z 297)

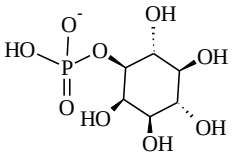

Inositol phosphate ion (m/z 241)

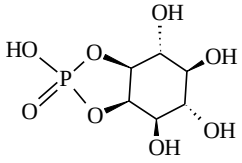

Inositol phosphate ion – H_2O (m/z 223)

***Table 2**. LIPID MAPS predicted fragments for PG as $[M-H]^-$ adduct ion in negative ionization mode*

Phosphatidylglycerol (PG)

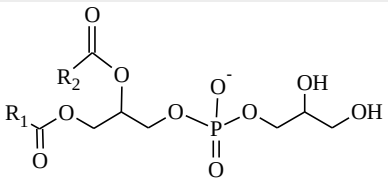

Phosphatidylgkycerol $[M-H]^-$

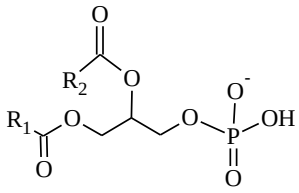

Loss of glycerol

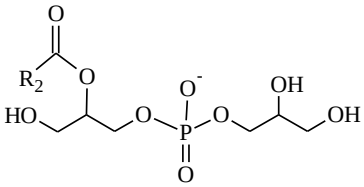

Loss of acyl chain (sn1) as ketene

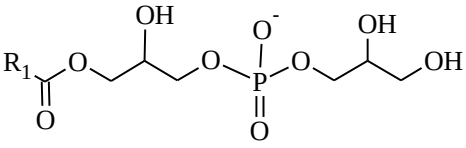

Loss of acyl chain (sn2) as ketene

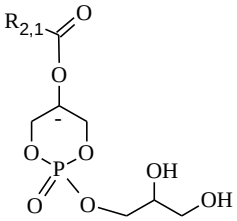

Neutral loss of RCOOH (sn1/sn2)

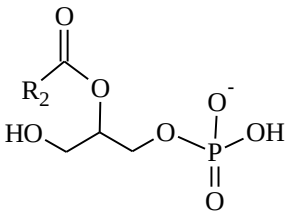

Sn1 loss of acyl chain as ketene and glycerol

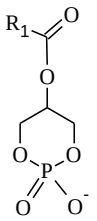

Neutral loss of sn2 acyl chain and glycerol

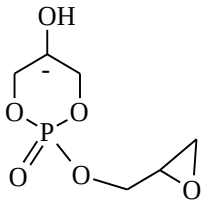

Glycerophosphoglycerol ion -2 H_2O

(m/z 209)

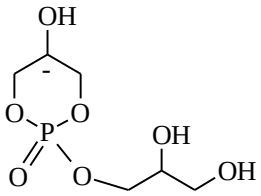

Glycerophosphoglycerol ion -H_2O

(m/z 227)

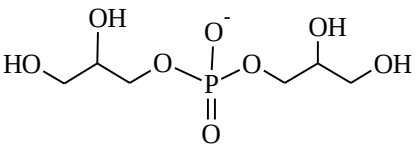

Glycerophosphoglycerol ion

(m/z 245)

1.6 Lipid Extraction

To perform glycerophospholipid analyses from biological samples a prior separation from other matrix constituents like proteins, carbohydrates and amino acids is required. For this purpose, liquid/liquid extraction procedures are commonly used. They involve diethyl ether, hexane, chloroform, methanol-chloroform or alcohol-ether as extraction agents.

Methods used by Bligh, Dyer and Folch are some of the most common and efficient methods for lipid extraction. They are also used today with promising reproducibility. In 1959 Bligh and Dyer proposed a lipid extraction from homogenized tissues with methanol-chloroform mixture. The extraction takes place in a monophasic system with proportions of methanol-chloroform which allow forming a miscible system with water from the tissue.[35] Folch used chloroform-methanol (2:1) mixture to extract lipids from homogenized brain tissue. Non-lipid substances were additionally washed with water.[36]

Bloor proposed an alcohol/ether extraction method for the determination of fat in small amounts of blood.[37] Moreover, in 1936 Boyd used the same alcohol/ether procedure to get better extraction efficiencies for phospholipids and free cholesterol in comparison to neutral fats and cholesterol esters.[38]

Extraction with hexane was also proposed as an efficient procedure for lipids from oil samples. For all extractions, the extract composition and lipid quantity content varies dependent on the temperature and liquid/liquid contact time. Using hexane, the amount of extracted phospholipids increases with increasing temperature, but at 60°C the phospholipid content suddenly reduces.[39]

Recently it is proposed an extraction with the methyl tert butyl ether (MTBE) as a simple, single-solvent extraction method. This approach is suitable for lipid extraction from cells, as well as fluids and tissues.[40] As a low-density organic solvent in comparison to chloroform containing extraction solvents, MTBE forms an upper organic layer after the phase separation, making sample collection simpler. Additionally, using MTBE reduces sample loss because there is no sample dripping. The formation of crude pellets in the extraction system and its removal by the centrifugation aids the sample collection step.

Two more advantages of using MTBE in the extraction procedure over Folch, Bligh and Dyer are better extraction recoveries and less toxicity for the experimentator as well as for the environment.

Comparing the MTBE extraction procedure with the one of the Folch, Bligh and Dyer, MTBE gives faster and higher recoveries for major lipid classes such as PE, PC, PI, ceramide (Cer),

cholesteryl ester (CE), sphingomyelin (SM) and diacylglycerol.[39] MTBE can also replace commonly used chloroform extraction procedures for tissue matrices which are demonstrated in the case of human and mouse brain.[40, 41]

1.7 Methodical approaches in Lipidomics

Lipids require reliable methods for their identification and quantification because of the structural similarities between compounds classified in different categories.

Considering recent technological advances this can be achieved with approaches based on mass spectrometric analysis with soft ionization techniques like electrospray ionization (ESI) and matrix-assisted laser desorption ionization (MALDI).

There are three main approaches in lipidomics mass spectrometry based on the sample introduction system:

1. Shotgun lipidomics employs a direct infusion of the whole lipid extract into the tandem mass spectrometer without prior separation. In this case, each compound identification can be confirmed with the fragmentation pattern in the MS/MS scans of the respective precursor ion. Shotgun lipidomics approach is briefly discussed in the section [1.8].

2. LC-MS/MS is based on chromatographic separation of analytes from the lipid extract prior introduction into the tandem mass spectrometer, in order to reduce sample complexity. This approach allows quantification and identification of lipids.

3. MALDI-based methods are mainly used for imaging biological tissues by resolving the special distribution of lipids and also give information about the lipid dynamics in tissues.

Lipidomics require sensitive, accurate and fast mass spectrometers with high mass resolution. Considering these requirements there is hardly any mass spectrometer designed to fulfill all these parameters. Triple quadrupole (QqQ) and QTRAP mass spectrometers have in comparison to other mass spectrometers, better sensitivity, selectivity and higher speed. Their only drawback is the low mass accuracy and resolution. Highly accurate mass spectrometers implemented for lipidomics analysis are time of flight (TOF) and orbitrap mass spectrometers.[42]

QqQ is already well established in lipidomics targeted approach for identification and quantification of phospholipids of different origin.[43, 44, 45] Lipidomic platforms based on QTRAP mass spectrometer analysis for profiling approach for phospholipids, sphingolipids, fatty acids[46] and eicosanoids was also developed.[47]

The family of orbitrap mass spectrometers has shown promising opportunities for determination of total lipid content in extracts from different origins. For the measurement of our samples, we used an ion trap-orbitrap tandem mass spectrometer for phospholipid identification. Orbitrap as the mass analyzer is appreciated for its high mass accuracy in the low ppm range.[48] This is beneficial and crucial for the characterization of the whole sample lipidome in a single run, considering a high number of different lipid categories with only minute mass differences.

For the characterization of the total lipidome diverse platforms with TOF, QTRAP, QqQ and orbitrap mass spectrometers were developed and described in section [1.8].

1.8 Shotgun lipidomics

Shotgun lipidomics, as one of three approaches for lipid identification (see section [1.7.]), allows very fast acquisition of the spectra from directly infused lipid extracts into the mass spectrometer without prior separation. It is less suitable for low abundant lipids. The ionization of low abundant lipids is suppressed due to high ion density in the ion source. To reduce the ionization suppression injection of smaller sample volumes are required. With the NanoMate Advion nano electrospray ionization source, a stable electrospray is established with just 5µl inlet volume (TriVersa User Training manual, 2009).

Shotgun lipidomics can be applied using both targeted and untargeted approaches. Targeted approaches are the more commonly applied methods in lipidomics and involve modes such as precursor ion scanning, neutral loss scanning, product ion scanning and multiple reaction monitoring. The advantages of targeted approach are in the application for high throughput analysis with high sensitivity, accuracy and precision.[42] Untargeted approaches are general methods to detect all lipids in the sample in a single run with a wide m/z range. This approach is not class specific and allows also the detection of novel lipids. The instruments used specifically for the untargeted approach are tandem mass spectrometers with high resolution and mass accuracy involving TOF and orbitrap mass analyzers. With the application of high-resolution MS1 and additional MS2 scans, the identification of isobaric species is possible.

Several shotgun lipidomics platforms were developed by different groups in the last years.

Multi-dimensional MS-based shotgun lipidomics,[49] is a lipidomic platform developed by Han's group. Xianlin Han, Ph.D. is a professor at the Sanford-Burnham Medical Research Institute (Florida, USA). His group introduced triple quadrupole tandem mass spectrometer (QqQ) to

acquire MS1 and MS2 lipid spectra applying a targeted approach in different scan modes. Scan modes used include product ion mode, neutral loss scanning mode, precursor ion scanning mode and multiple reaction monitoring. For each scan type, in multidimensional lipid mapping method, m/z values of fragments are plotted against m/z values of precursor ions. This method was proven also for quantitative approaches and is in detail described by Han.[49]

AB Sciex developed a methodology similar to Han`s platform: Total ion mapping by using quadrupole time of flight mass spectrometer (QqTOF) via infusion MS/MS^{ALL} workflow for lipids.[50] QqTOF is here presented with mass resolutions of over 30 000 and mass accuracy of 2 ppm.[50] Analysis results are represented in the form of 3D generated contour plots with precursor masses (quad) plotted against fragment masses (TOF), allowing better visualization of precursor and fragment distributions as well as neutral losses and characteristic fragments for lipid classes. Lipid identification is performed with LipidView™ software involving the lipid fragment database. This software possesses a tool to filter neutral losses or fragments from the experimental data set.[50]

Targeted approaches which were used by Hahn and AB Sciex are not suitable for the detection of novel lipids. This disadvantage was overcome by developing a high-resolution tandem mass spectrometry platform by Andrej Shevchenko. Shevchenko's platform introduced the high mass resolution shotgun lipidomics on the hybrid linear trap-orbitrap tandem mass spectrometer.[1] Additionally, he used the Advion Triversa NanoMate® as a nano flow ion source and LipidXplorer to automatically perform the lipid identification of shotgun spectra.

1.8.1. Ion source

Soft ionization techniques such as electrospray ionization (ESI) are important in mass spectrometry-based lipidomics approaches to obtain information of intact lipid masses.

The continuous electrospray in the ESI source plays a crucial role for the mass spectrometric analysis and therefore the sample should be consistently delivered with constant flow rates. Initially, syringe pumps and autosamplers were used as a sample delivery system.[42] However, it was shown that these techniques suffer from some difficulties for automatization, considering high flow rates in µl/min range.

First automated approaches were developed after the introduction of a nano flow electrospray ion source. Triversa NanoMate® (Advion) is a chip based technology, allowing nano flow electrospray ionization with three different operation modes: LESA (Liquid surface extraction analysis), LC/MS fraction collection/infusion and chip-based infusion. For shotgun lipidomics the chip-based infusion mode has most extensively been applied. In the chip-based infusion mode sample delivery to the MS instrument is performed via the robotic pipette tip holder of NanoMate®. After sample aspiration in the µl volume range (5 µl to 10 µl), the pipette tip loaded with sample moves towards and ESI chip at the mass spectrometer inlet. The voltage applied on the tip causes the formation of a nano flow electrospray that is introduced into the mass spectrometer.

***Figure 8**. Inner part of the Advion Triversa NanoMate®: On the bottom are tip wrack (left) and 384-well well plate (right). The well plate is positioned on a plate cooler allowing temperatures from 4°C to 25°C. Above is a robotic part of the NanoMate® for sample collection and transport to ESI chip.*

The NanoMate® is controlled by the ChipSoft software, which allows optimization of several parameters like the spray current and the backpressure (described briefly in section [2.1]). Additionally, the written sequence offers in the ChipSoft a good opportunity to make this process automatic. The selection of well plate type material depends on the sample type, with maximal 20 mm plate height, as recommended from Advion. For lipids the most suitable well

plates to our knowledge are Eppendorf Twin-Tec 96- or 384-well, V-bottomed, skirted plate, with adhesive aluminum sealing tape, compatible with organic solvents such as chloroform.

The pipette tips used in NanoMate® system are made of impregnated conductive carbon material preventing oxidation that can occur after the high voltage is applied on the carbon material. After every sample delivery, the pipette tip is exchanged with a new one.

The ESI Chip is a miniaturized electrospray ionization source, consisting of a 400 nozzle array for nano-electrospray ionization (see **Figure 9**). There are different ESI chip types, fabricated with different nozzle diameters depending on the applied infusion flow rate and they are visually distinguishable by color: dark blue (A-Chip), light blue (D-Chip) and red (G-Chip). Dark blue A-Chip (see **Figure 9**) is recommended for general purpose and all applications, with the largest possible nozzle diameter of 5,5 µm compatible for infusion rates of 100 –500nL/min.[51] Other ESI chip types are compatible if lower flow rates are required and have smaller nozzle diameters.

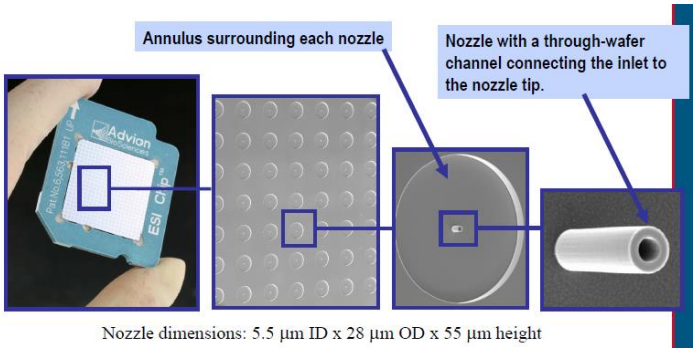

Figure 9. *Advion ESI Chip* [51]

For every run, the NanoMate® picks a new pipette tip from the tip holder prior to the sample aspiration and uses a separate nozzle in the ESI-Chip. In such manner, a sample to sample carryover is prevented. With adequately adjusted back pressure and voltage, constant electrospray can be generated. The values for pressure and voltage depend on the sample matrix type, the voltage polarity, the type and the concentration of added buffer (see section [2.2.3]).

1.8.2 Orbitrap tandem mass spectrometer

The sample is introduced from the ion source into the mass spectrometer after the ionization process. The aim of the mass spectrometric analysis is to analyze intact masses of lipids (parent ions) and identify them with the following fragmentation step. Therefore, acquisition of MS1 and MS2 spectra is required for the exact identification and characterization of lipid analytes, which is achieved by applying two different analyzers in the hybrid mass spectrometer.

In shotgun lipidomics, several types of mass spectrometers have found application, such as QqQ, QTRAP, TOF and orbitrap.[42] The lipidomics platform of Shevchenko's laboratory introduced the orbitrap family into the shotgun lipidomics world. Shevchenko used an LTQ-Orbitrap XL™ mass spectrometer for high-throughput analysis by coupling it with a TriVersa NanoMate® Advion nano ion source.[52, 53] This method shows potential to be optimized on the LTQ-Velos™ Hybrid Ion Trap-Orbitrap Mass Spectrometer physically coupled to the ETD module. These instruments are quite similar. Both are equipped with two analyzers: the ion trap and the orbitrap. The only hardware differences are that the LTQ-Velos™ has an extra ETD fragmentation module and a dual cell two-dimensional linear ion trap. On the other hand, the LTQ-Orbitrap XL™ contains a single cell two-dimensional linear ion trap.

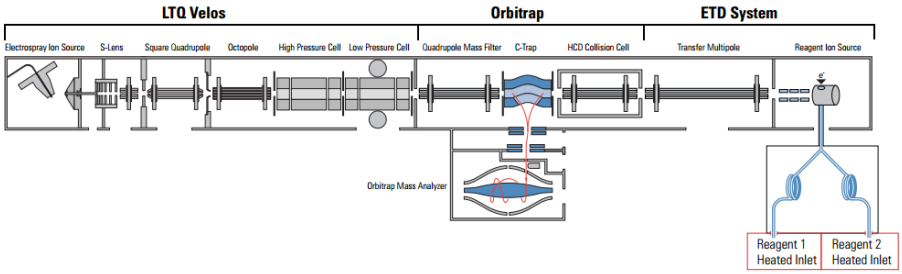

Figure 10. *LTQ-VelosTM incl. ETD module*[54]

The combination of the accurate and high resolving orbitrap mass analyzer for the MS and the dual cell linear ion trap for the MS2 acquisition allows generating accurate MS spectra with fast MS2 screening. Although, there are several ways to perform MS2 analysis on the LTQ-Velos mass spectrometer, considering the different variety of possible fragmentation opportunities and MS analyzer combinations.

The LTQ-Velos™ instrument consists of three main modules: LTQ Velos, Orbitrap and ETD system. Ionized samples are firstly introduced into the LTQ-Velos module. This module contains the dual cell ion trap as independent MS analyzer for fast screening. The introduced ion beam is focused with an S-lens and transferred via square quadrupole and octapole to the

dual cell ion trap. The mass analyzer in the LTQ module consists of two linear ion trap cells and three metal lenses (front, center and back) which provide conductance limits.[54] These lenses are located prior, between and after the ion trap cells. The ion trap allows screening of precursor ions by specific m/z values, which can be used in the MS1 scanning mode. Furthermore, it is used for isolation, ion trapping and fragmentation of precursor ions with collision induces dissociation (CID) in the MS2 scanning mode. For the following detection, the SEM detector or the orbitrap can be used.

The orbitrap module consists of an octapole, a c-trap, z-lenses, a HCD collision cell and the orbitrap mass analyzer itself. After passing through the LTQ module, ions are transferred via octapole and collected in the c-trap via specifically applied RF values. The c-trap is gas filled, providing the necessary environment to damp high kinetic energy of entered ions and keep them in the center of the c-trap. The orbitrap analyzer is applicable both in MS1 and MS2 experiments. In the MS1 experiment, the ion beam is transferred intact through the LTQ module and collected in the c-trap. Such collected ions are directly introduced into the orbitrap passing the z-lenses which provide spatial focusing of the ion beam. In the MS2 experiment already fragmented ions are transferred into the orbitrap. The fragmentation can be proceeded with collision-induced dissociation (CID) in the ion trap, higher-energy collisional dissociation (HCD) in the HCD collision cell and electron transfer dissociation (ETD) in the ETD module. The CID is performed in the LTQ-Velos module with the following ion beam transport via octapole and c-trap into the orbitrap. The HCD fragmentation occurs in the HCD collision multipole cell filled with a collision gas. After entering the HCD cell, parent ions are brought to fragmentation through the collision with the gas. Further, fragment ions are transferred back into the c- trap via an applied potential gradient and then into the orbitrap mass analyzer. The ETD fragmentation occurs in the ETD module, which is physically coupled to the orbitrap module and is used for higher charge state ions and big molecules such as proteins and peptides.[55] In ETD module external anions are applied to transfer an electron onto the peptide

cation and to form a peptide radical. ETD fragmentation results in c- and z-ions causing not the peptide bond to break but C-terminal to the amino group.[56]

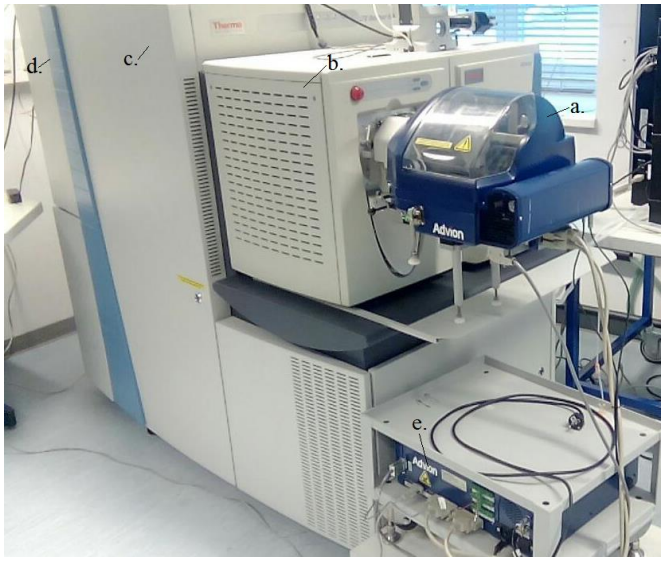

Figure 11. *LTQ-Velos™ Hybrid Ion Trap-Orbitrap Mass Spectrometer physically coupled to the ETD module. a) TriVersa NanoMate® Advion, b) LTQ Velos module, c) Orbitrap module, d) ETD system module, e) Interface to link the mass spectrometer, the NanoMate® and the computer together.*

1.8.3 Interpretation of lipid MS spectra

It has been considered that lipids are a vast heterogenic group of biomolecules, with different ionization properties and instrument dependent fragmentations.[32,33] This shows the importance for developing an automated lipid identification software. The most frequently occurring problems in shotgun lipidomics are the absence of appropriate software and algorithms for the automated identification. Some software versions are available for free, such as LipidXplorer[57] and ALEX[58]. The lipid platform of Shevchenko introduced LipidXplorer for the lipid identification from shotgun spectra. The function of this software is based on self-written queries which are used to navigate the interpretation of imported spectra in LipidXplorer. The queries include also theoretically proposed fragments of MS2 spectra. The workflow of LipidXplorer identification can be described in five steps:

*1. Generation of shotgun tandem mass spectra as a lipidomic data set (**.mzXML file) – The import module of the LipidXplorer converts raw spectra files into an *.mzXML file. Here raw spectra represent MS2 spectra of technical replicates for the respective sample.

2. Import tandem mass spectra in LipidXplorer as MasterScan – In the MasterScan (flat file database) MS peaks in the *.mzXML file are aligned and merged to generate a representative aligned peak data set for the specific sample. This is done by a specific averaging algorithm [59] were also MS2 spectra are associated with corresponding precursor ions from the aligned MS1.

3. Writing of MFQL Queries - interpretation queries written in MFQL (molecular fragmentation query language) language serve as self-generated MS lipidomic data bank with fragments for specific lipids and LipiExplorer interpretation workflow.

4. Search of experimental spectra (in form of MasterScan) according to written MFQL queries

5. Output information as .csv file which is supported by Microsoft Excel

The function and the workflow of LipidXplorer is in detail described by Herzog.[59]

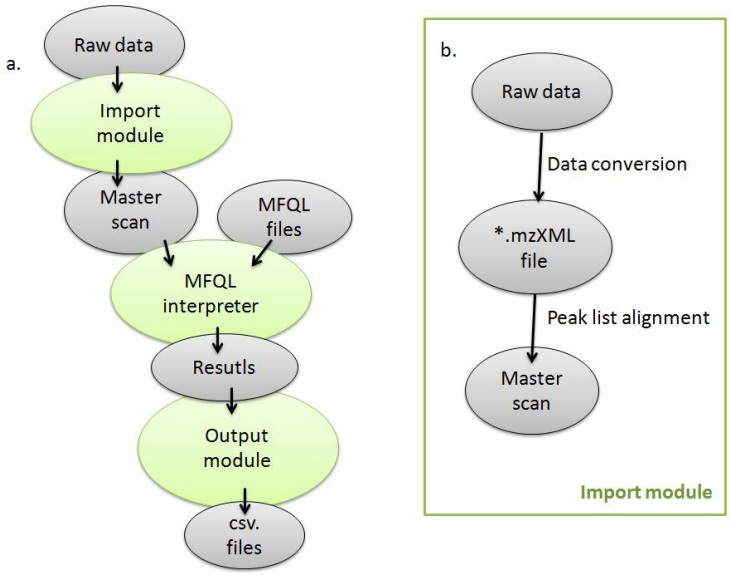

Figure 12. *Workflow of LipidXplorer. a) LipidXplorer operation. In green are three main functional modules presented. Between the modules in blue illustrated is the data flow. Import module which converts raw data into the MasterScan (flat file database). b) Generation of the MasterScan (flat file database) in the LipidXplorer.*

Lipid Explorer as a lipid identification and characterization open source software can be downloaded from the wiki site: https://wiki.mpi-cbg.de/lipidx/Main_Page. Additionally, MFQL files for different phospholipid classes used for lipid identification in the bovine heart[59] in E.*Coli*[59] and in human blood plasma[60] are available.

2. Methods

Chemicals, standards, and instruments are listed in the appendix.

Amnion biopsy and pig lung lavage samples were provided by Angela Lemke Ms.C. from the Ludwig Boltzmann Institute for experimental and clinical Traumatology in Vienna. The cultivation procedures were performed in the Ludwig Boltzmann Institute for experimental and clinical Traumatology.

2.1 MTBE Extraction

Preparation for the MTBE Extraction.

One aliquot of amnion and pig lung lavage samples were extracted on the same day after being obtained from the Ludwig Boltzmann Institute for Experimental and Clinical Traumatology. The rest was frozen and stored at – 90°C. For further use, the frozen samples were defrosted at room temperature for 30 min on the Thermomixer prior the extraction procedure. High temperatures were avoided to prevent degradation processes.

Methyl-tert-butyl-ether extraction procedure.

- 200 µl of the sample was placed in an Eppendorf Tube (2ml).
- 320µl of methanol (97%) was further added to the sample and is vortexed shortly.
- For the extraction 1ml of the MTBE was added to the sample and the mixture was mixed for 1h at 20°C and 1400 rpm in the Thermomixer.
- 250 µl of H_2O was afterward added to achieve phase separation.
- The mixture was centrifuged for 1 min at 4000 rpm and the upper organic phase (800µl) was collected in a glass vial.
- Such prepared sample extracts were stored at -20°C prior the measurement.

The workflow of the MTBE extraction is represented in **Figure 13**.

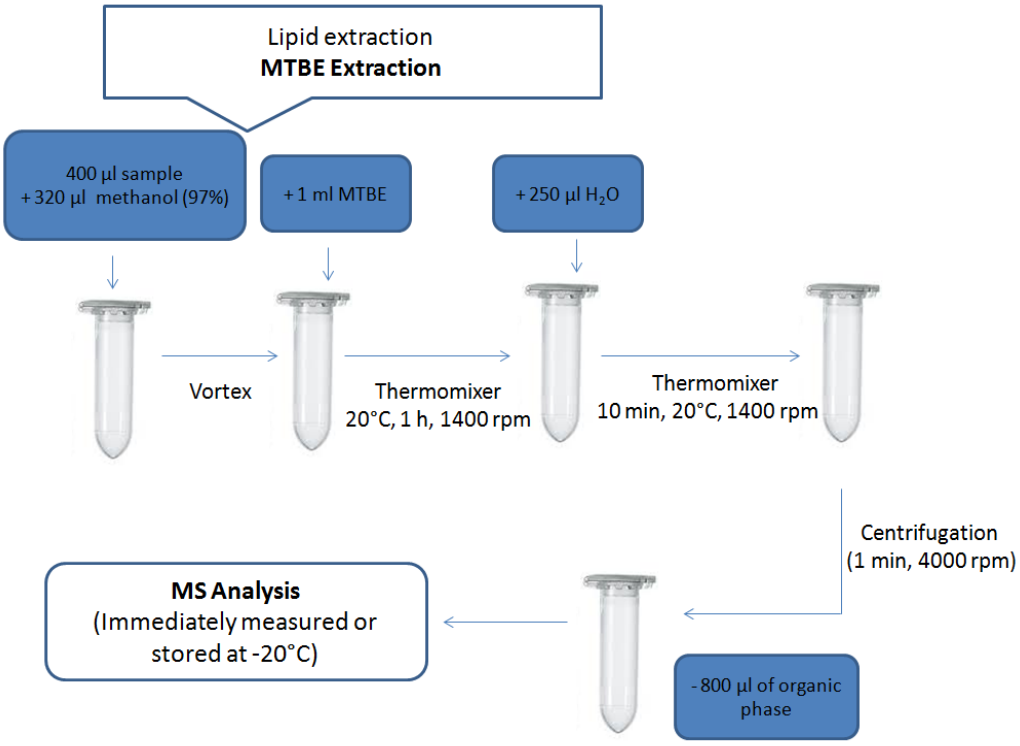

Figure 13. *Overview of the MTBE lipid extraction procedure*

2.2. Mass spectrometric analysis

The mass spectrometric analysis was performed on the LTQ-Velos, a hybrid ion-trap orbitrap mass spectrometer equipped with TriVersa NanoMate® as a nano ion source. To generate a nano-electrospray ionization, we used Advion A-Chip with 400 nozzles and 5,5 µm nozzle diameter.

The samples are loaded into the wells of 384-well and 96-well plates. Each loaded well contained 8µl of the MTBE lipid extract and 80 µl of the solvent.

We have set 5 µl as an aspiration volume for every run. The ionization process was performed for 5 min in the nano-ESI Chip with a constant sample delivery. As a result, an electrospray is generated which is constantly delivered into the mass spectrometer.

We performed mass spectrometric measurements for both polarity modes and achieved to generate an incessant electrospray with a constant flow rate. This is essential to perform a high throughput analysis. Constant flow rates were accomplished by separating both polarity measurements in two different runs. In contrary, our attempts failed to perform a switching polarity measurement that was described in Shevchenko work.[52] The most essential here is to

adjust the solvent composition that allows measurements and an electrospray with constant flow in both polarity modes. The advantage of the polarity switch is to make the screening method faster, due to the possibility to acquire positive and negative ion mass spectra in a single run. It is demonstrated that orbitrap requires 90 min to stabilize the sensitivity and the accuracy in the low ppm range after the polarity switch.[51] Further, NanoMate® requires some period of time to exchange the pipette tip, to aspirate the sample and that the pipette tip engages the ESI Chip. However, to separately perform both polarity measurements, we adjusted two compositions of the solvent mixture (see section [2.2.1]).

Lipid identification and characterization requires information of theoretical fragments. These are commonly gained from the reference standard MS2 spectra of each lipid, respectively. Such generated spectra would be in the case of shotgun lipidomics expensive and are therefore not recommended. Another possibility is the LIPID MAPS with a developed tool to perform the theoretical lipid fragmentation. Unfortunately, this is possible for lipids measured in the negative ion mode. Due to the lack of theoretical fragment information's which would make an automate lipid identification possible, we have faced difficulties to interpret experimental generated positive mass spectra. Therefore, we decided after numerous attempts to carry out and implement an automated method for phospholipid identification in the negative ion acquisition mode, with CHCl3/MeOH (3/7, v/v) solvent mixture buffered with 7,5mM ammonium acetate. The automated identification is performed with the LipidXplorer software, which contains theoretical phospholipid fragmentation patterns of lipids in queries. These fragment patterns are obtained from the LIPID MAPS identification tool (LIPID MAPS online tools for lipid research, 2007).

We used several optimization steps which are described in following sections to automate the mass spectrometric analysis. To carry out the mass spectrometric analysis it is important to write suitable methods that control separately the ion source and the mass spectrometer.

Generally, in this work optimization comprises the adjustment of buffered solvent composition [2.2.1] to applied back pressure and voltage in the nano-electrospray ionization source of TriVersa NanoMate® Advion. This optimization step requires special attention for optimization because it provides the formation of analyte ions which are essential to perform mass spectrometric analysis at all. The method for the ionization source process is written in the software Chipsoft 8.3.1 and is detail discussed in section [2.3.1].

Next step to be considered is the mass spectrometric measurement on the LTQ-Velos hybrid instrument. Operations in the mass spectrometer are already automated and require just a specification of the process. We specified parameters for the mass spectrometric operations in the Thermo software. They depend on the sample type and the type of desired information

in the tandem mass spectra. Some of these parameters are the selection of the mass analyzer for MS1 and MS2 performance, m/z for precursor ion isolation and fragmentation type and fragmentation energy (see section [2.3.2]).

After the ionization step, both processes should be timely adjusted during the run, in order to quantitatively introduce the ions into the mass spectrometer. This is possible via the contact closer signal in the Chipsoft 8.3.1 software.

2.2.1 Solvents for shotgun measurement

The measurements for both polarity modes were performed as separated runs with different solvent compositions. The measurement in the positive ion mode was accomplished with $CHCl_3$/MeOH/Isopropanol (1/2/4, v/v/v) and in negative ion mode with $CHCl_3$/MeOH (3/7, v/v). Both solvents mixtures were buffered with 7,5 mM ammonium acetate.

The initial aim was to optimize the polarity switching mode on the LTQ Velos mass spectrometer. Therefore, we performed mass spectrometric measurements with the same solvent composition which is mentioned by Schuhmann.[52] Applying same voltage and backpressure parameters and using the solvent composition as described in the publication, we could generate a positive electrospray with a constant flowrate in the nano-electrospray ionization source. In contrast, measurements in negative ionization mode after many attempts showed some issues with the electrospray. Electrospray drop could be observed soon as the ionization process started. We decided to perform the run in the negative ion mode without isopropanol, as we observed that the isopropanol causes the electrospray drop. The optimization of the solvent composition in negative ionization mode is described section [2.2.2].

2.2.2 Optimization of solvent composition in the negative ion mode

The solvent mixture that consists of methanol and chloroform contributed to uninterrupted flow rates by the negative electrospray. According to this, we tried to optimize the proportions of methanol and chloroform which give minimum fluctuations in the electrospray.

For this purpose, we prepared a series of eleven solvent mixtures with varied portions of methanol and chloroform and buffered them with 7,5 mM ammonium acetate. These solvent mixtures are listed in **Table 3**.

To observe the negative electrospray trend from all solvents, the wells of the 384-well plate were successively loaded with the solvent mixtures. The mass spectrometric measurements in the negative polarity mode were performed on the LTQ-Velos^{TM} mass spectrometer. The LTQ-Velos was equipped with the TriVersa NanoMate® that serves as the nano-electrospray ionization source. ChipSoft 8.3.1 is a specially designed software to control the functional parameters under which NanoMate® operates. The nano-electrospray ionization was set for 5 min with 1.20 psi for backpressure and 1.42 kV for voltage. Under this conditions, ChipSoft 8.3.1 was monitoring in real time the electrospray current for each solvent mixture. This could be observed as a displayed plot of the current [nA] and the time [min] in a separate window.

Table 3. *Variations of solvent mixtures proved for the most constant electrospray in nano-ESI source*

#	MeOH [%]	$CHCl_3$ [%]
1	100	0
2	90	10
3	80	20
4	70	30
5	60	40
6	50	50
7	40	60
8	30	70
9	20	80
10	10	90
11	0	100

Figure 14 represents experimental obtained electrospray current profiles for all eleven solvent mixtures which are numbered from one to eleven. On the first glance, the fluctuation in the electrospray current can be observed for every solvent. Generally, fluctuations are caused by the presence of air bubbles in the solvent. They can be avoided with the prior vortexing step.[61] We were not interested in that clean results so we skipped it.

Finally, we chose the solvent mixture at the position four which consists of 70% methanol, 30 % chloroform and 7,5 mM ammonium acetate, considering to have the most constant electrospray trend when compared with other. For further mass spectrometric analysis, we always used this solvent mixture composition for all samples.

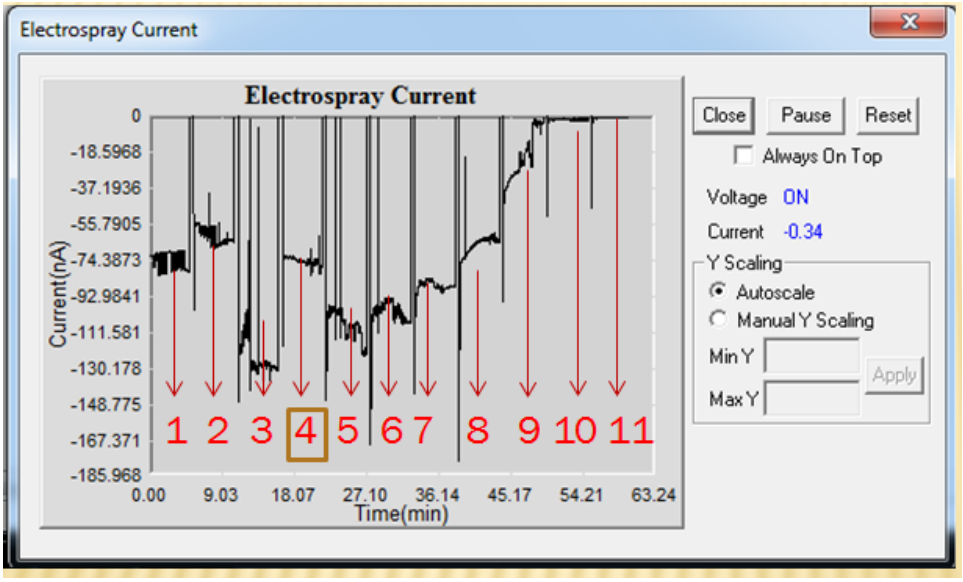

Figure 14. *Electrospray current for eleven solvent mixtures with varying portions of chloroform and methanol. The numbers correspond to the solvent mixtures in* ***Table 3***

2.2.3. Nanoflow ion source

To generate an electrospray with nano-flow, we used TriVersa NanoMate® Advion in a chip-based infusion mode which is coupled to the LTQ-Velos tandem mass spectrometer (see sections [1.8.2] and [1.8.3]).

2.2.3.1 ChipSoft 8.3.1 software

In this section more attention is dedicated to basic operations in the ChipSoft 8.3.1 software, that we used to operate the ionization processes in the TriVersa NanoMate® in order to generate a good electrospray current prior the mass spectrometric measurement.

Getting the NanoMate® ready for measurement. Two routine tests were performed every day prior the measurement and involve the chip alignment and the manual centering of the pipette tip at the mass spectrometer inlet.

Chip alignment is an operation controlled via ChipSoft 8.3.1, which automatically aligns the nozzles of the nano-ESI chip with the pipette tip and the mass spectrometer inlet. The alignment is recommended always after the NanoMate® is uncoupled and again coupled to the LTQ-Velos mass spectrometer. For safety reasons, we did the chip alignment every day in the morning briefly before the measurement. In ChipSoft 8.3.1 chip alignment is commanded in the interface settings tab by pressing chip alignment bottom. This process comprises a 10 min alignment test with following alignment process that lasts 20 min. The NanoMate® automatically stops the process after the alignment test, if the chip is already aligned.

Numerous runs affect some hardware failures that cannot be avoided and afford manual correction. Pipette tip in the off-center of the mass spectrometer inlet is an example. Therefore, we routinely centered the pipette tip every morning or sometimes twice a day via navigation bottoms in spray optimization window of the ChipSoft 8.3.1 software.

Method Parameters to be considered. In ChipSoft 8.3.1 method parameter specifications and conditions under which NanoMate® operates are located in the method manager tab (see **Figure 15**). Method manager is divided into six main sections:

1. Method information
2. Sample information
3. Advanced parameters
4. Temperature
5. Spray parameters

6. Spray sensing

Section *sample information* allows the definition of the aspirated sample volume in the pipette tip on the robotic part of the NanoMate® as well the opportunity to return the unused sample in the well. We defined 5µl as an aspiration volume for every used method. The NanoMate® has also an additional opportunity to use vent headspace or to aspirate air after sample. This is an advantage in case of heavy samples with very low surface tensions and therefore prevents sample dripping prior the pipette tip engages the chip. For instance, this is a favorable tool if solvents with high portions of chloroform are used.

In the *temperature* section, it is possible to define the temperature of a cooler block placed under the well plate. In the very beginning, we did an inconsiderate step and performed measurements at 4°C to prevent solvent evaporation. Here, more attention is afforded by temperature selection. Temperatures under 12°C cause condensation of water from air into the sample and result fluctuations in the electrospray. Therefore, all following measurements were performed at temperatures above 12°C. In order to minimize the solvent evaporation as well as the water condensation, additionally, we used suitable aluminum plate seals to cover the loaded wells of the well plate. In the *advanced parameters* section, there is a Pre-Piercing parameter and should be turned on if plate seals are used. Under this condition NanoMate® is commanded to pierce the seal of the target well prior sample aspiration with defined Pre-Piercing depth given in mm. This section gives also an opportunity to navigate the automate start of mass spectra acquisition with applying the contact closure signal for the mass spectrometer.

The *spray sensing* sections are used to command the NanoMate® to change the nozzle if spray current falls under a predefined value of voltage. This operation was not used in our measurements.

If the parameters in these sections except *spray parameters* are once defined, they show no need to be changed for further analysis. The *spray parameters* section allows the definition of the sample acquisition time, the applied voltage, the backpressure and the acquisition polarity. We experienced a different quality of the electrospray for the same sample that is measured on different days at the same voltage and backpressure conditions. However, if the electrospray current showed with already used method a bed trend, we have pressed the spray optimization bottom for manual spray optimization. This allows optimizing the electrospray current with the adjustment of voltage and backpressure without acquisition of MS spectra. The newly changed parameters can be applied to the method after pressing the “Apply Values To Method” bottom.

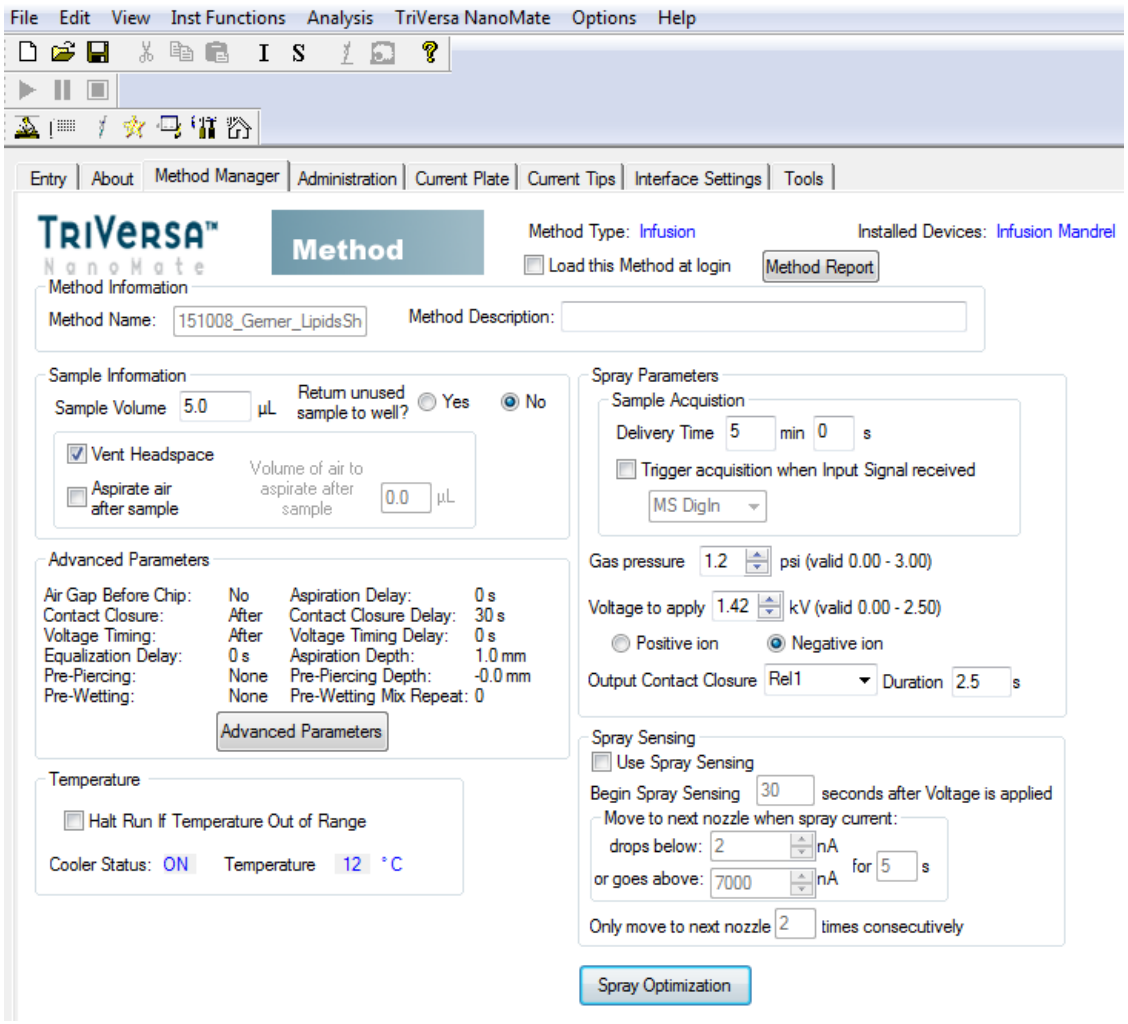

Figure 15. *Method manager tab in ChipSoft 8.3.1 software*

2.2.3.2 Method parameters for nano-electrospray ionization

In order to generate a constant electrospray with nano-flow, we performed mass spectrometric analysis with different method parameters for the nano ionization source. The parameters for the gas pressure and the applied voltage were varied in the Chipsoft 8.3.1 software. Here, we present three methods for the nano ion source (see **Table 4**). The sample volume, the ionization polarity, and the sample delivery time are commonly defined parameters for all used methods. In contrast to the gas pressure, the applied voltage on the pipette tip and the temperature of a cooling block located under the loaded well plate.

Initially, the measurements were performed with loaded 384-well plates. Afterward, we switched to 96-well plates which allow additional sample preservation with an aluminum foil cover. This cover provides good ambient to cool the samples at 12°C and to prevent changes

in the sample composition due to the solvent evaporation or the water condensation from the air. Each method is characterized by some advantages and disadvantages. Hence, in the performed automated measurements they are proven as reliable.

Properties of Methods 1 and 2:

+ no need to use an aluminum foil as cover (fewer costs)
+ more space for samples (384 wells)
- very low temperatures can cause water condensation from air and bubbles in the electrospray

Properties of Method 3:

+ aluminum foil prevents solvent evaporation, therefore, at the same time the sequence are more samples listed
+ at 12°C no water condensation
- less space for samples (96 wells)

***Table 4**. Defined parameters for used methods in negative ionization mode*

Chipsoft 8.3.1 to control Triversa nanomate (Advion)							
Method	Gas Pressure	Voltage to apply	Temepratu re	Sample Volume	Polarity	Delivery Time	Well plate
1	1.20 psi	1,42 kV	4°C	5µl	Negative	5 min	384
2	0,3 psi	1,40 kV	4°C	5µl	Negative	5 min	384
3	1,1 psi	1,1 kV	12°C	5µl	Negative	5 min	96

2.3.2 LTQ Velos mass spectrometer

To operate the mass spectrometric process in the hybrid LTQ-Velos mass spectrometer, we used the XCalibur™ software from Thermo Fisher Scientific. The aim of this work was to optimize a method for a reliable and an automated mass spectrometric measurement of phospholipids on the LTQ-Velos tandem mass spectrometer equipped with TriVersa NanaMate® as the nano ion source.

Table 5. *MS1 and MS2 Method Parameters for LTQ Velos hybrid mass spectrometer*

LTQ Velos		
MS1		**MS2**
Analyzer	Orbitrap	Ion trap
Mass Range	200-1000 Th	200-700 Th
Scan Type	Full	Dependent top 10 or top 6
Polarity	Positive / Negative	Positive/negative
Resolution	100000	
Acquire Time	4,5 min	
Lock Mass	529,4629	

Table 5 presents a rough overview of used method parameters for MS and MS2 acquisitions of the MTBE lipid extracts. To perform an MS analysis, we selected the orbitrap analyzer to acquire accurate full scan MS1 spectra of parent ions, with resolving power of 100 000 m/z at 400 m/z. MS spectra are acquired within an m/z mass range of 200-1000. After lock mass introduction at 529,4629 m/z for real-time mass calibration, we acquired mass spectrometric spectra within 5 ppm mass accuracy. In total LTQ-Velos needs 4.5 min to precede one run and acquire at least 300 MS spectra.

The MS2 acquisition is performed by dual cell ion trap analyzer which allows fast screening of the fragment ions. Engaging the MS2 dependent scan in the setup tab of XCalibur, the LTQ-Velos isolated for fragmentation via collision induced dissociation (CID), the predefined 6, 8 or 10 most intense precursor ions. The isolated precursor ions had 1 m/z width in the former acquired MS spectrum. We set 40eV for normalized collision energy which is sufficient to perform a full fragmentation process within 10 ms of activation period (see **Figure 16**).

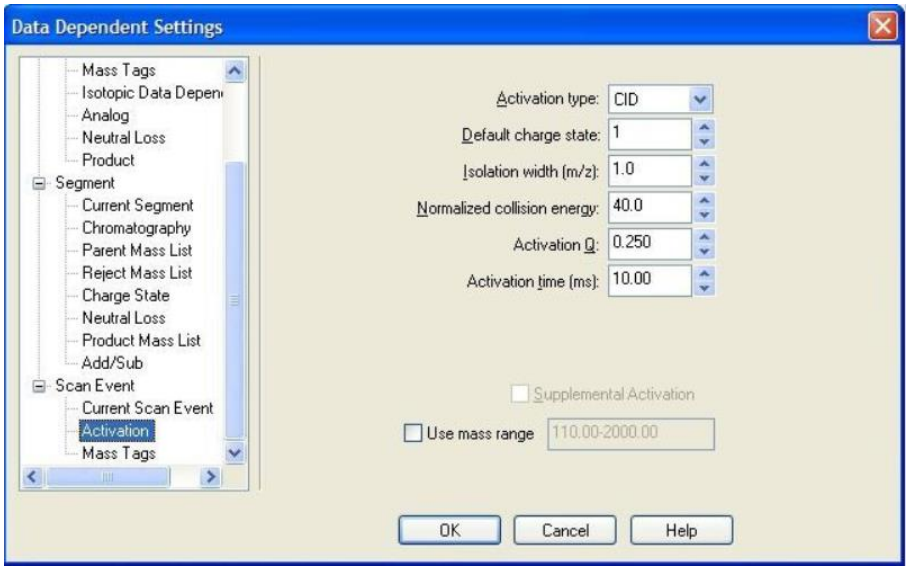

Figure 16. *Fragmentation parameters in the Data Dependent Settings window for of XCalibur ™ (Thermo Fisher Scientific)*

The dynamic exclusion list is in our method enabled in order to minimize the fragmentation of same precursor ions of recurring mass spectrometric measurements. Therefore, the precursor ion after triggered MS2 scan is put in the exclusion list for some predefined period and is excluded from repeated MS2 analysis. This parameter is especially important while performing shotgun experiments, considering a vast amount of different compounds which are present in the full scan MS1 spectrum. On this way also less abundant precursor ions have a higher opportunity to be fragmented. We used 270 s for exclusion duration with one repetition count and 20 s repeat duration. In addition, we set 1m/z for the exclusion mass width and did not enable early expiration (see **Figure 16**).

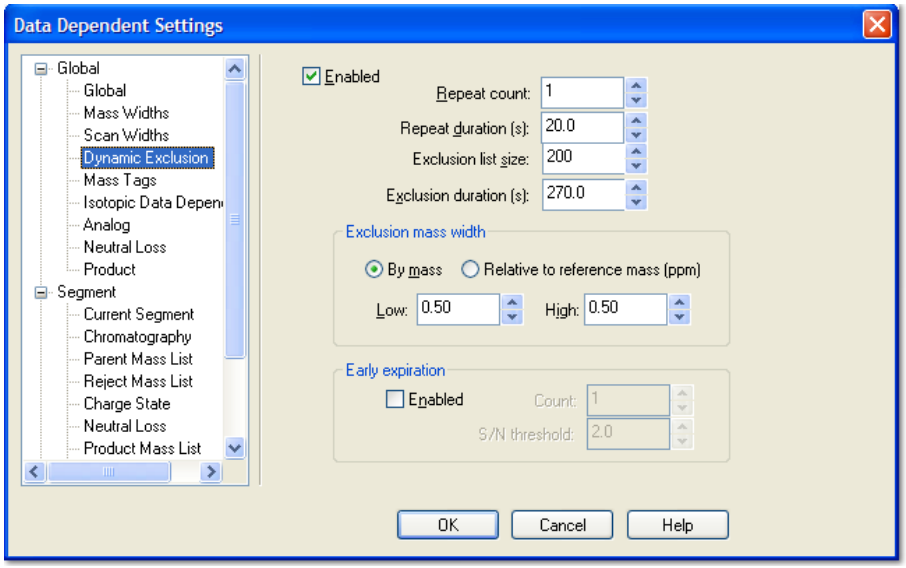

Figure 17. *Dynamic exclusion parameters in Data Dependent Settings window of XCalibur TM (Thermo Fisher Scientific)*

Hence, as we were interested in precursor ions in one charged state, we enabled the monoisotopic precursor selection and charge state screening parameter to reject 2 and higher charge states.

After repetitive mass spectrometric measurements of our MTBE lipid extracts, we could characterize phospholipids that are present in our sample. Therefore, in the data dependent window of XCalibur™, we created a parent ion list with m/z values of already found phospholipids. This makes for further analysis, on the one hand, the fragmentation of desired precursor ions selective which are sometimes less abundant. On another hand, the fragmentation is for the mass spectrometer simpler and smaller MS spectra files are generated. As expected, we observed no peaks in MS2 spectra after fragmentation of precursor ions with MS intensities under a distinct threshold of E2. This is in consequence of inevitable losses during the ion transport and the fragmentation process. Precursor ion peaks with intensities over this threshold lead to fragment ion peaks in MS2 spectra, with the intensity difference of two decimal units when the precursor ion is compared with his highest fragment ion. This was tested while performing two runs with the enabled and the disabled parameter in the Data Dependent Settings window which stands for “Fragmentation of the most intense peak from MS spectrum if no Parent Masses are found” (see **Figure 18**). If this parameter is disabled, then less abundant precursor masses were skipped and the most intense fragmented.

To detect novel lipids, precursor ion lists should be avoided in the mass spectrometric method while performing the shotgun lipidomics approach. Therefore, as the phospholipid composition in the MTBE lipid extracts were determined, we used the targeted approach just to reduce the number of unwanted MS2 spectra and generate more technical replicates for the LipidXplorer.

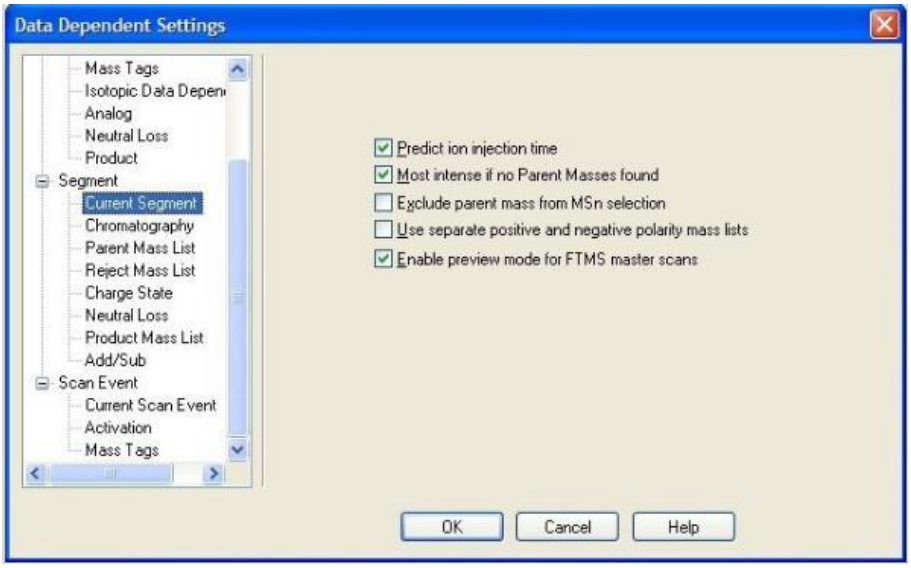

***Figure 18**. Data Dependent Settings window of XCalibur TM (Thermo Fisher Scientific)*

3.Results

3.1 Lipidomics profiling in Amnion

We investigated the lipid profile of the amnion biopsy secretome as MTBE extract. Therefore, amnion biopsies from two distinct regions in the amniotic sack were used: placental amnion part (P) and the reflected part located opposite to the placenta (RA). Each biopsy was cultivated in the DMEM (D) and the SAGM (S). Specific probes of both cultivation media which contain supernatant lipids were extracted with the MTBE. In total, we had four types of supernatant MTBE extracts: PS, PD, RAS and RAD. The PS and the RAS are probes derived from the SAGM, whereas the PD and the RAD are derived from the DMEM cultivation medium. For further information, such as altering lipid profiles by different individuals, we used also amnion biopsy samples from two donors numbered with 23 and 24.

Table 6 shows all lipid species in MTBE lipid extracts obtained after the mass spectrometric measurement. Additionally, detected lipid species in amnion samples were associated into five phospholipid subclasses: sphingomyelins (SM), phosphatidylcholines (PC), phosphatidylserines (PS) and phosphatidylethanolamines with ester linkage (PE) and with ether linkage (PE-O). They show a clear tendency to give always the same type of adduct ion for the same subclass. The PE-O and the PS prefer to build deprotonated adducts $[M-H]^-$, in contrast, SM, PC and PE were found in mass spectra as acetate adducts $[M+OAc]^-$.

Furthermore, we observed that fatty acyl chains of phospholipids were unsaturated and saturated with 1,2,4 and 5 double bonds consisting of 16, 18, 20 and 22 carbons.

Data evolution was proceeded in such manner to observe the impact of the cultivation medium and the type of amnion biopsy on the lipid secretion.

Table 6. *Phospholipid species observed in FTMS spectra in the supernatant of the amnion biopsy and the characteristic adduct ions for the phospholipid subclasses*

Subclass	Species		Adduct ion
PE-O	[34:2]	[16:1 / 18:1]	$[M-H]^-$
	[36:5]	[16:1 / 20:4]	$[M-H]^-$
	[38:6]	[16:1 / 22:5]	$[[M-H]^-$
	[38:6]	[18:2 / 20:4]	$[[M-H]^-$
	[38:5]	[18:2 / 20:3]	$[M-H]^-$
	[38:5]	[16:0 / 22:5]	$[M-H]^-$
	[38:5]	[16:1 / 22:4]	$[M-H]^-$
	[38:5]	[18:1 / 20:4]	$[M-H]^-$
SM	[34:1]	-	$[M+OAc]^-$
	[36:1]	-	$[M+OAc]^-$
	[42:2]	-	$[M+OAc]^-$
	[42:1]	-	$[M+OAc]^-$
PC	[32:0]	[16:0 / 16:0]	$[M+OAc]^-$
	[34:1]	[18:1 / 16:0]	$[M+OAc]^-$
	[36:1]	[18:0 / 18:1]	$[M+OAc]^-$
	[38:4]	[20:4 / 18:0]	$[M+OAc]^-$
PE	[36:2]	[18:1 / 18:1]	$[M+OAc]^-$
	[38:1]	[20:0 / 18:1]	$[M+OAc]^-$
PS	[36:1]	[18:1 / 18:0]	$[M-H]^-$
	[36:0]	[18:0 / 18:0]	$[M-H]^-$

The total sum of lipid species in samples for each donor and subclass is demonstrated in **Table 7**. Additionally, for better data visualization the same results can be seen as a plot in **Figure 19**.

Table 7. *Total sum of lipid species for both donors after experimental MS data evaluation*

Donor		**23**	**24**	**Total number of lipids in both donors**
Sample types		**Number of lipids pro donor**		
RAD	**PE-O**	15	22	**37**
	SM	12	24	**36**
	PC	12	24	**36**
	PE	5	11	**16**
	PS	5	11	**16**
RAS	**PE-O**	4	21	**25**
	SM	4	6	**10**
	PC	8	13	**21**
	PE	-	1	**1**
	PS	2	7	**9**
PD	**PE-O**	20	33	**53**
	SM	12	24	**36**
	PC	12	24	**36**
	PE	6	12	**18**
	PS	6	12	**18**
PS	**PE-O**	14	42	**56**
	SM	6	13	**19**
	PC	7	15	**22**
	PE	-	4	**4**
	PS	3	10	**13**

In **Table 7** the PD is demonstrated with the highest number of lipid species, whereas RAS was found as lipid-poor. In general, we observed that samples derived from DMEM cultivation medium, such as the PD and the RAD, contained more lipid species than the corresponding

from SAGM. The SAGM cultivation medium contributes in some way to the decrease of lipid species in RAS and PS samples. This is demonstrated in **Figure 19** for all subclasses except for PE-O. The PS sample is found to be rich with PE-O species.

Further comparisons were performed to investigate the impact of the amnion biopsy on the phospholipid profile. The amnion biopsy from the placental side (P) has shown to be more favorable for lipid secretion. The RA was generally found poor with lipid species (see **Figure 19**).

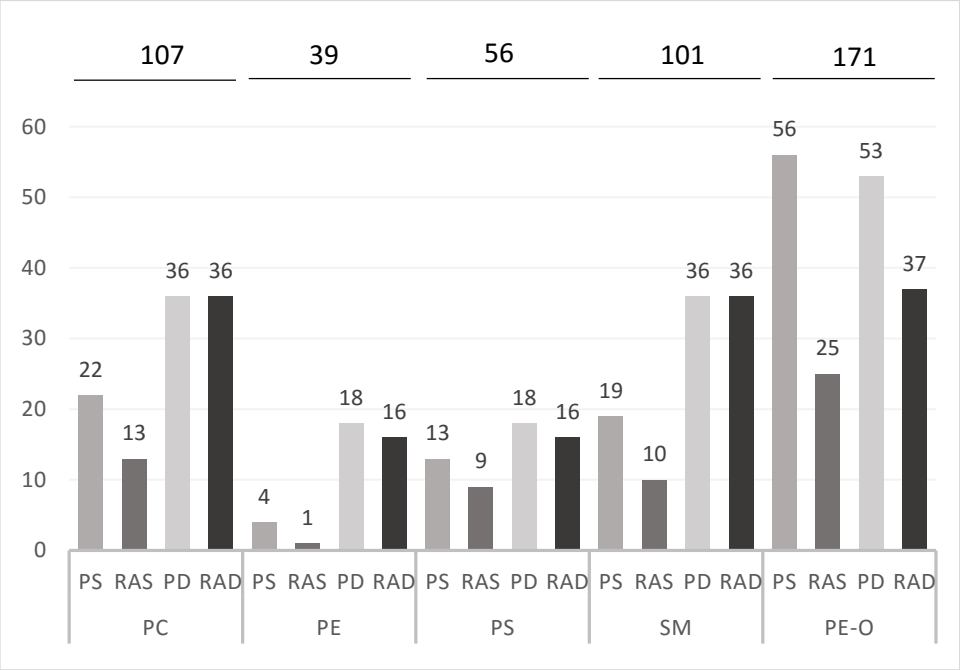

Figure 19. *Total sum of supernatant lipids within a subclass observed by both donors and at all cultivation times.*

Figure 19 demonstrates a phospholipid distribution overview of subclasses in all sample types.

The aim was to accomplish a better and simpler visualization of results. For this purpose, we summed all found lipids from one subclass which are found in one sample type. The distribution of phospholipid species within each sample is discussed in sections [3.1.1-3.1.4].

PE-O is with 171 lipids, the most prominent subclass and is mostly present in the PS sample. Other subclasses were found mostly in the PD. This makes PE-O in comparison to other subclasses specific.

PC was found to be the subclass with the greatest number of identified phospholipids with 107 IDs followed by SM with 101, PS with 56 and PE with 39 lipids.

Generally, PD and RAD samples were observed as lipid rich in contrary to PS and RAS samples. Furthermore, the total number of lipids was determined to be higher in PD than in RAD samples. The same applies for PS and RAS samples.

Next to be observed is the lipid distribution compared between the different samples (see **Figure 19**). The PE-O subclass was to the greatest extent contained in the PD and is followed by SM and PC with 36 lipids, and PE and PS with 18 lipids. Same distribution trend is observed in the RAD. In RAS and PS again the highest number of lipids was showed for the PE-O and decreases in series with PC, SM, PS and PE.

Same results could be obtained after individual observation of phospholipid subclasses in samples. This is represented in percentage terms in **Figures 20,21,22** and **23**.

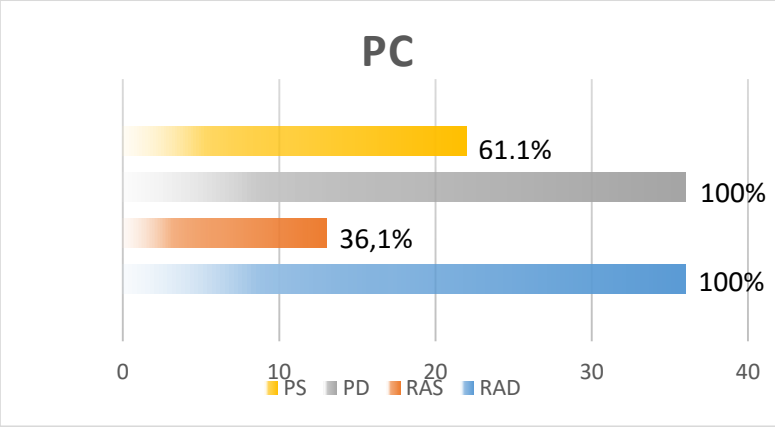

***Figure 20**. Percentages of PC lipids compared to the total number of common lipid species for this subclass in PS, PD, RAS and RAD samples considering all incubation times and both donors*

Considering the total number of lipids, phosphatidylcholine is after PE-O on the second place. The distribution of PC lipids within the sample type is demonstrated in **Figure 20**. It can be observed that PD and RAD samples contained all common PC lipids for this subclass. Whereas, the PS and the RAS, shared 61% and 36% of common lipids.

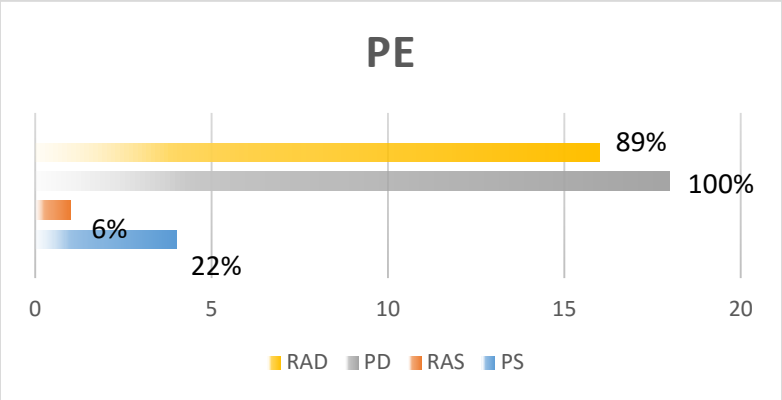

Figure 21. *Percentages of PE lipids compared to the total number of common lipid species for this subclass in PS, PD, RAS and RAD samples considering all incubation times and both donors*

The distribution of PE lipids in the amnion samples is similar to the one of the PC, as demonstrated in **Figure 21**. 100% of common PE lipids were only found in PD samples, and slightly less in the RAD. The RAS shared just 6% of them which corresponds to one PE [36:2] lipid. Considering this results, PE subclass showed the smallest number of lipids.

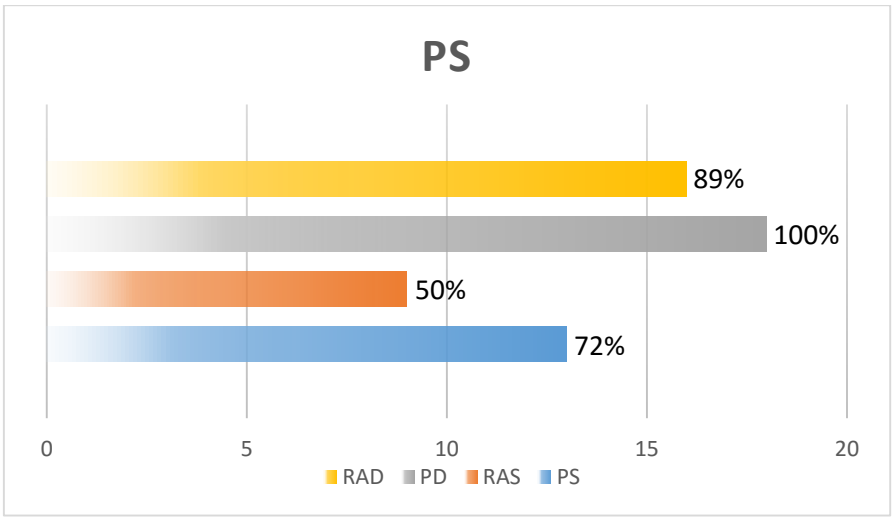

Figure 22. *Percentages of PS lipids compared to the total number of common lipid species for this subclass in PS, PD, RAS and RAD samples considering all incubation times and both donors*

In total, 56 of phosphatidylserine lipids were found in all samples. 18 of them are contained in the PD samples, which makes 100 % of common lipids for the PS subclass (see **Figure 22**). 89% of common lipids were found in RAD samples corresponding to 16 lipids. Phosphatidylserine subclass is poorer in amnion samples cultivated in the SAGM medium (PS and RAS).

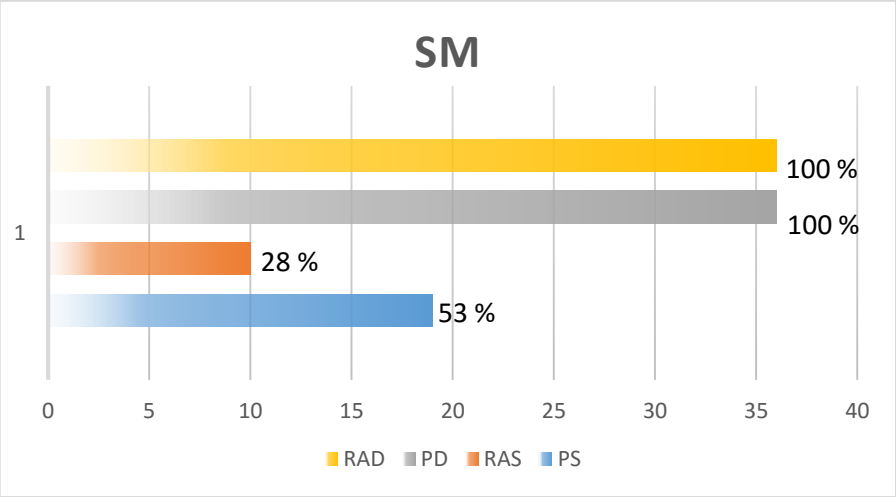

Figure 23. *Percentages of SM lipids compared to the total number of common lipid species for this subclass in PS, PD, RAS and RAD samples considering all incubation times and both donors*

RAD and PD samples were found with same number of SM lipids. Each sample contained 36 lipids which represent 100% of the subclass specific lipid content. In contrast, the PS and the RAS were not rich with SMs. The PS sample contained 19 lipids (53%) and the RAS sample 10 (28%) (see **Figure 23**).

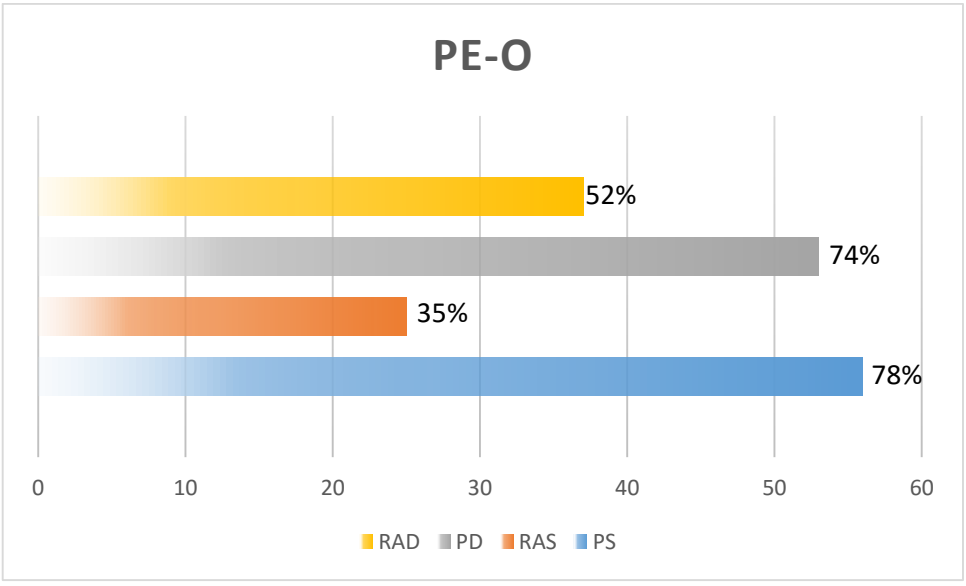

Figure 24. *Percentages of PE-O lipids compared to the total number of common lipid species for this subclass in PS, PD, RAS and RAD samples considering all incubation times and both donors*

Considering the total subclass specific lipid content, PE-O was shown as the richest. In total, 171 lipids were found for the PE-O subclass in all samples (see **Figure 19**).

As previously seen, all subclasses showed their highest lipid content in PD samples. However, we have found that the PE-O subclass was most enriched in PS samples (see **Figure 24**). Of total 171 PE-O lipids in all samples, 56 were present in the PS sample representing 78% of common PE-O lipids. Additionally, **Figure 24** shows less PE-O lipid content in the RAD (52%) and the RAS (35%) samples.

3.1.1 The total number of lipid species in supernatants of amnion biopsy

Table 8 represents the total number of lipid species which were found in the supernatant of different amnion biopsies from two donors. Generally, PD and RAD samples are prior demonstrated to contribute more lipids than the RS and RAS. The distribution has the same trend in case of the lipid species.

The highest number of lipid species was found in the PE-O subclass with 8 common lipid species. Almost every common PE-O was in all samples of the PS present. In total 4 PC species in the supernatant of amnion biopsy were found. All 4 species are contained in every PD and RAD sample, regardless of the donor and the cultivation time. In the RAS and the PS, fewer PCs are noticeable. Same applies for the SM subclass.

In contrary, species of PE and PS subclasses were less present. In both subclasses, just 2 species were found. Both are in every PD sample contained. The RAD mainly contains both species in its samples. The PE species were completely absent in the PS and RAS samples of donor 23 and 24. Additionally, the same was demonstrated for PS by donor 23.

The lowest number of found lipids were demonstrated in the RAS whereas the PE subclass contributed the lowest number of lipid species.

3.2 Lipidomics profiling in pig lavage

Table 13. *Lipid species of six lipid classes observed in FTMS spectra from lipid extracts of pig lavage. Dark blue shadowed boxes represent lipid species with an error under five ppm and the light blue boxes the one above five ppm. With red are marked phospholipids which contain fatty acyl chains with odd number of carbon atoms and with blue the one found additionally with the manual spectra interpretation.*

Lipid class	Species		Adduct ion
LPC	[16:0]	[16:0]	$[M+OAc]^-$
PC	[34:0]	[18:0 / 16:0]	$[M+OAc]^-$
PC	[30:0]	[14:0 / 16:0]	$[M+OAc]^-$
PC	[32:2]	[14:0 / 18:2]	$[M+OAc]^-$
PC	[32:0]	[16:0 / 16:0]	$[M+OAc]^-$
PC	[33:1]	[17:1 / 16:0]	$[M+OAc]^-$
PC	[36:3]	[18:2 / 18:1]	$[M+OAc]^-$
PC	[38:1]	[18:0 / 20:1]	$[M+OAc]^-$
PC	[32:2]	[16:1 / 16:1]	$[M+OAc]^-$
PC	[36:4]	[20:4 / 16:0]	$[M+OAc]^-$
PC	[36:2]	[18:1 / 18:1]	$[M+OAc]^-$
PC	[36:2]	[18:2 / 18:0]	$[M+OAc]^-$
PG	[36:1]	[18:1 / 18:0]	$[M-H]^-$
PG	[38:5]	[18:1 / 20:4]	$[M-H]^-$
PG	[32:0]	[16:0 / 16:0]	$[M-H]^-$
PG	[36:2]	[16:0 / 20:2]	$[M-H]^-$
PG	[34:2]	[16:0 / 18:2]	$[M-H]^-$
PG	[34:2]	[18:1 / 16:1]	$[M-H]^-$
PG	[32:1]	[16:0 / 16:1]	$[M-H]^-$
PG	[32:1]	[18:1 / 14:0]	$[M-H]^-$
PG	[34:1]	[16:1 / 18:0]	$[M-H]^-$
PG	[34:1]	[16:0 / 18:1]	$[M-H]^-$
PG	[36:2]	[18:1 / 18:1]	$[M-H]^-$

PG	[36:2]	[18:0 / 18:2]	$[M-H]^-$
PE	[32:0]	[16:0 / 16:0]	$[M+OAc]^-$
PE	[32:0]	[18:0 / 14:0]	$[M+OAc]^-$
PE	[34:1]	[18:1 / 16:0]	$[M+OAc]^-$
PE	[34:1]	[16:1 / 18:0]	$[M+OAc]^-$
PE	[36:2]	[18:1 / 18:1]	$[M+OAc]^-$
PE	[38:4]	[18:1 / 20:4]	$[M+OAc]^-$
PS	[38:4]	[18:0 / 20:4]	$[M-H]^-$
PS	[34:1]	[16:1 /18:0]	$[M-H]^-$
PS	[36:1]	[18:1 / 18:0]	$[M-H]^-$
PS	[40:1]	[18:1 / 22:0]	$[M-H]^-$
PE-O	[40:5]	[18:1 / 22:4]	$[M-H]^-$
PE-O	[38:5]	[18:1 / 20:4]	$[M-H]^-$
PE-O	[38:5]	[16:0 / 22:5]	$[M-H]^-$
PE-O	[38:5]	[16:1 / 22:4]	$[M-H]^-$
PE-O	[36:5]	[16:1 / 20:4]	$[M-H]^-$
PE-O	[37:4]	[21:4 / 16:0]	$[M-H]^-$
PE-O	[41:6]	[19:1 / 22:5]	$[M-H]^-$
PE-O	[39:5]	[21:4 / 18:1]	$[M-H]^-$
SM	[34:1]		$[M+OAc]^-$

3.1.2 Lipidomics profiling of PDs

Table 8. *Green boxes highlight the presence of lipid species in the PD samples. Found lipid species are associated with following subclasses: phosphatidylethanolamines with ether linkage (PE-O) and ester linkage (PE), sphingomyelins (SM), phosphatidylserines (PS) and phosphatidylcholines (PC). Lipids were determined from two donors 23 and 24, after cultivation of their amnion biopsies for 2, 3, 4 and 7 days in the DMEM medium. The medium was changed at different times, every 27, 40, 45, 48 and 55 hours.*

PD	Donor		23			24					
	Days of incubation		2	3	7	2	2	4	4	7	7
	Time without medium change		27	40	45	48	48	48	48	55	55
	Diameter of biopsy plate					2 cm	8 mm	2 cm	8 mm	2 cm	8 mm
PE-O	[34:2]	[16:1 / 18:1]									
	[36:5]	[16:1 / 20:4]									
	[38:6]	[16:1 / 22:5]									
	[38:6]	[18:2 / 20:4]									
	[38:5]	[18:2 / 20:3]									
	[38:5]	[16:0 / 22:5]									
	[38:5]	[16:1 / 22:4]									
	[38:5]	[18:1 / 20:4]									
SM	[34:1]										
	[36:1]										
	[42:2]										
	[42:1]										
PC	[32:0]	[16:0 / 16:0]									
	[34:1]	[18:1 / 16:0]									
	[36:1]	[18:0 / 18:1]									
	[38:4]	[20:4 / 18:0]									
PE	[36:2]	[18:1 / 18:1]									
	[38:1]	[20:0 / 18:1]									
PS	[36:1]	[18:1 / 18:0]									
	[36:0]	[18:0 / 18:0]									

The distribution of phospholipid species in PD samples is demonstrated in **Table 9**. The biopsies from two donors were cultivated for 2, 3, 4, and 7 days and the medium was changed after every defined period as given in **Table 9**.

Common lipid species for subclasses SM, PC, PE and PS were fully present in samples from both donors and at all incubation times. In contrast, PE-O showed a slight difference to other subclasses, concerning the presence of lipid species. It can be seen that the cultivation times are partially related to the lipid content in case of the PE-O subclass (see **Table 9**). Additionally, the diameter of the biopsy plates showed influence on the species content. More secreted species are found in the samples cultivated in biopsy plates with 2 cm of diameter than in the case of 8mm. The sample with 27h of incubation time and two incubation days from donor 23 showed fewer PE-O species than the one incubated longer e.g. three and seven days. Similarly, it is observed for samples from donor 24. On the day seven, donor 24 secreted in 55h all common PE-O species, whereas on the day four and two the number of secreted species in 48h is lower.

In total, PD showed more lipid species in samples with longer incubation days as well as times between the medium change.

3.1.3 Lipidomics profiling of PS

In contrast to PD samples, **Table 10** demonstrates that PS samples generally contained fewer lipid species for all subclasses and the lipid content varied from subclass to subclass. The PE-O was more prominent than the other. Some subclass species were completely absent in specific samples, e.g. PE in all samples from donor 23.

In donor 23, a higher number of lipid species for all subclasses was observed in samples with longer cultivation times. Therefore, the sample from day seven contained more lipid species than the other two with shorter incubation periods. On the day two the biopsy from donor 23 secreted in 27h just two lipid species: the SM [34:1] and the PS [34:1].

Unlikely, donor 24 showed a random lipid distribution, considering the cultivation times. We observed also a variation of the lipid content between samples in both biopsy plates. For instance, the species distribution in samples with two and four incubation days and a cultivation period of 48h (see **Table 10**).

***Table 10**. Green boxes highlight the presence of lipid species in PS samples. Found lipid species are associated with following subclasses: phosphatidylethanolamines with ether linkage (PE-O) and ester linkage (PE), sphingomyelins (SM), phosphatidylserines (PS) and phosphatidylcholines (PC). Lipids were determined from two donors 23 and 24, after cultivation of their amnion biopsies for 2, 3, 4 and 7 days in SAGM medium. The medium was changed at different times, every 27, 40, 45, 48 and 55 hours.*

PS			Donor	23			24					
			Days of incubation	2	3	7	2	2	4	4	7	7
			Time without medium change	27	40	45	48	48	48	48	55	55
			Diameter of biopsy plate				2cm	8mm	2cm	8mm	2cm	8mm
PE-O	[34:2]	[16:1 / 18:1]										
	[36:5]	[16:1 / 20:4]										
	[38:6]	[16:1 / 22:5]										
	[38:6]	[18:2 / 20:4]										
	[38:5]	[18:2 / 20:3]										
	[38:5]	[16:0 / 22:5]										
	[38:5]	[16:1 / 22:4]										
	[38:5]	[18:1 / 20:4]										
SM	[34:1]											
	[36:1]											
	[42:2]											
	[42:1]											
PC	[32:0]	[16:0 / 16:0]										
	[34:1]	[18:1 / 16:0]										
	[36:1]	[18:0 / 18:1]										
	[38:4]	[20:4 / 18:0]										
PE	[36:2]	[18:1 / 18:1]										
	[38:1]	[20:0 / 18:1]										
PS	[36:1]	[18:1 / 18:0]										
	[36:0]	[18:0 / 18:0]										

3.1.4 Lipidomics profiling of RAD

Table 11. *Green boxes highlight the presence of lipid species in RAD samples. Found lipid species are associated with following subclasses: phosphatidylethanolamines with ether linkage (PE-O) and ester linkage (PE), sphingomyelins (SM), phosphatidylserines (PS) and phosphatidylcholines (PC). Lipids were determined from two donors 23 and 24, after cultivation of their amnion biopsies for 2, 3, 4 and 7 days in DMEM medium. The medium was changed at different times, every 27, 40, 45, 48 and 55 hours.*

RAD		Donor	23			24					
		Days of incubation	1	7	3	2	2	4	4		
		Time without medium change	27	45	40	48	48	48	48	55	55
		Diameter of biopsy plate				2 cm	8 mm	2 cm	8 mm	8 mm	2 cm
PE-O	[34:2]	[16:1 / 18:1]									
	[36:5]	[16:1 / 20:4]									
	[38:6]	[16:1 / 22:5]									
	[38:6]	[18:2 / 20:4]									
	[38:5]	[18:2 / 20:3]									
	[38:5]	[16:0 / 22:5]									
	[38:5]	[16:1 / 22:4]									
	[38:5]	[18:1 / 20:4]									
SM	[34:1]										
	[36:1]										
	[42:2]										
	[42:1]										
PC	[32:0]	[16:0 / 16:0]									
	[34:1]	[18:1 / 16:0]									
	[36:1]	[18:0 / 18:1]									
	[38:4]	[20:4 / 18:0]									
PE	[36:2]	[18:1 / 18:1]									
	[38:1]	[20:0 / 18:1]									
PS	[36:1]	[18:1 / 18:0]									
	[36:0]	[18:0 / 18:0]									

Table 11 indicates the distribution of phospholipid species in RAD samples in different incubation periods. Both donors were rich with SM and PC species and contained all common species of the respective subclasses.

The PE-O species were not present in the sample from donor 23 cultivated for 27 h. The same could be observed in the PS (see **Figure 10**). In contrast, longer cultivated samples from the incubation day three and seven were rich with species from this subclass. Generally, donor 24 was also found poor with PE-O in comparison to the total number of common PE-O species. Almost all common PE and PS species were present in samples of both donors.

The diameters of biopsy plate have an influence on the lipid profile. Namely, at same incubation times, we could observe different phospholipid profiles. For instance, samples from donor 24 which are cultivated for 48h and 55 h.

Table 12 indicates a very poor phospholipid distribution for all subclasses in RAS samples. The RAS is in comparison to other sample types poor and showed a non-uniform distribution of lipids at different incubation times and in both biopsy plates. In contrast to other subclasses, the PE was not present in samples of donor 23.

In general, a direct relation between the species content and the cultivation time for all sample types was not observed. The lipid content in PD, PS and RAD was shown roughly dependent on the cultivation time, whereas the content in the RAS was not. The diameter of the biopsy plate and the respective subclass contributed also to this relation.

3.1.5 Lipidomics profiling of RAS

Table 12. *Green boxes highlight the presence of lipid species in RAS samples. Found lipid species are associated with following subclasses: phosphatidylethanolamines with ether linkage (PE-O) and ester linkage (PE), sphingomyelins (SM), phosphatidylserines (PS) and phosphatidylcholines (PC). Lipids were determined from two donors 23 and 24, after cultivation of their amnion biopsies for 2, 3, 4 and 7 days in the SAGM medium. The medium was changed at different times, every 27, 40, 45, 48 and 55 hours.*

RAS													
	Donor	23			24								
	Days of incubation	1	3	7	D	2	2	4	4	7	7		
	Time without medium change	27	40	45	48	48	48	48	48	55	55		
	Diameter of biopsy plate				2cm	2cm	8mm	2cm	8mm	2cm	8mm		
PE-O	[34:2]	[16:1 / 18:1]											
	[36:5]	[16:1 / 20:4]											
	[38:6]	[16:1 / 22:5]											
	[38:6]	[18:2 / 20:4]											
	[38:5]	[18:2 / 20:3]											
	[38:5]	[16:0 / 22:5]											
	[38:5]	[16:1 / 22:4]											
	[38:5]	[18:1 / 20:4]											
SM	[34:1]												
	[36:1]												
	[42:2]												
	[42:1]												
PC	[32:0]	[16:0 / 16:0]											
	[34:1]	[18:1 / 16:0]											
	[36:1]	[18:0 / 18:1]											
	[38:4]	[20:4 / 18:0]											
PE	[36:2]	[18:1 / 18:1]											
	[38:1]	[20:0 / 18:1]											
PS	[36:1]	[18:1 / 18:0]											
	[36:0]	[18:0 / 18:0]											

3.2 Lipidomics profiling in pig lavage

Table 13. *Lipid species of six lipid classes observed in FTMS spectra from lipid extracts of pig lavage. Dark blue shadowed boxes represent lipid species with an error under five ppm and the light blue boxes the one above five ppm. With blue are marked phospholipids additionally found with the manual spectra interpretation.*

Lipid class	Species		Adduct ion
LPC	[16:0]	[16:0]	$[M+OAc]^-$
PC	[34:0]	[18:0 / 16:0]	$[M+OAc]^-$
PC	[30:0]	[14:0 / 16:0]	$[M+OAc]^-$
PC	[32:2]	[14:0 / 18:2]	$[M+OAc]^-$
PC	[32:0]	[16:0 / 16:0]	$[M+OAc]^-$
PC	[36:3]	[18:2 / 18:1]	$[M+OAc]^-$
PC	[38:1]	[18:0 / 20:1]	$[M+OAc]^-$
PC	[32:2]	[16:1 / 16:1]	$[M+OAc]^-$
PC	[36:4]	[20:4 / 16:0]	$[M+OAc]^-$
PC	[36:2]	[18:1 / 18:1]	$[M+OAc]^-$
PC	[36:2]	[18:2 / 18:0]	$[M+OAc]^-$
PG	[36:1]	[18:1 / 18:0]	$[M-H]^-$
PG	[38:5]	[18:1 / 20:4]	$[M-H]^-$
PG	[32:0]	[16:0 / 16:0]	$[M-H]^-$
PG	[36:2]	[16:0 / 20:2]	$[M-H]^-$
PG	[34:2]	[16:0 / 18:2]	$[M-H]^-$
PG	[34:2]	[18:1 / 16:1]	$[M-H]^-$
PG	[32:1]	[16:0 / 16:1]	$[M-H]^-$
PG	[32:1]	[18:1 / 14:0]	$[M-H]^-$

PG	[34:1]	[16:1 / 18:0]	$[M-H]^-$
PG	[34:1]	[16:0 / 18:1]	$[M-H]^-$
PG	[36:2]	[18:1 / 18:1]	$[M-H]^-$
PG	[36:2]	[18:0 / 18:2]	$[M-H]^-$
PE	[32:0]	[16:0 / 16:0]	$[M+OAc]^-$
PE	[32:0]	[18:0 / 14:0]	$[M+OAc]^-$
PE	[34:1]	[18:1 / 16:0]	$[M+OAc]^-$
PE	[34:1]	[16:1 / 18:0]	$[M+OAc]^-$
PE	[36:2]	[18:1 / 18:1]	$[M+OAc]^-$
PE	[38:4]	[18:1 / 20:4]	$[M+OAc]^-$
PS	[38:4]	[18:0 / 20:4]	$[M-H]^-$
PS	[34:1]	[16:1 /18:0]	$[M-H]^-$
PS	[36:1]	[18:1 / 18:0]	$[M-H]^-$
PS	[40:1]	[18:1 / 22:0]	$[M-H]^-$
PE-O	[40:5]	[18:1 / 22:4]	$[M-H]^-$
PE-O	[38:5]	[18:1 / 20:4]	$[M-H]^-$
PE-O	[38:5]	[16:0 / 22:5]	$[M-H]^-$
PE-O	[38:5]	[16:1 / 22:4]	$[M-H]^-$
PE-O	[36:5]	[16:1 / 20:4]	$[M-H]^-$
PE-O	[37:4]	[21:4 / 16:0]	$[M-H]^-$
PE-O	[41:6]	[19:1 / 22:5]	$[M-H]^-$
PE-O	[39:5]	[21:4 / 18:1]	$[M-H]^-$
SM	[34:1]		$[M+OAc]^-$

Table 13 demonstrates lipid species which are contained in the pig lung lavage. The list is generated after experimental data evaluation of three biological replicates with repeated mass spectrometric measurements. Further, the identified lipid species in **Table 13** are obtained after manual and automatic data evaluation of respective MS spectra. The automatic one was performed via LipidXplorer with predicted fragmentation patterns from the LIPID MAPS (LIPID MAPS online tools for lipid research).

The type of the adduct ion that is formed in the ion source depends on the respective phospholipid subclass and is therefore subclass specific. We found PC, SM and PE to form acetate adduct ions $[M\text{-}OAc]^-$ in the ESI source, whereas PG, PS and PE-O tend to form deprotonated one $[M\text{-}H]^-$.

The subclass with the highest number of lipid species in the pig lavage was the PG. In the MTBE lipid extract of pig lavage, we have found 12 different species, which differ by the type of fatty acid esterified to the glycerol scaffold in the phospholipid.

The PC is in the second place considering the number of lipid species with 11 species. The expected DPPC which contains saturated fatty acyl chains with 16 carbons, as the most important one in this analysis, was also found with an error of 1,4 ppm. For a proper lung function, essential are also PC species which contain unsaturated fatty acids 14:0 (myristic acid) 16:0 (palmitic acid) and saturated acid 16:1 (palmitoleic acid).[62] We have found in the pig lung lavage two PC species which correspond to PC [14:0 / 16:0] and PC [16:1 / 16:1].

The PE-O is found with 8 different species. Further, it is followed by PE, PS and SM. We have found PE with 6, PS with 4 and SM with just 1 species.

The fatty acyl chains in phospholipids were found to contain mostly 14, 16, 18, 20, 22 as well as 15,17 and 19 carbon atoms. The acyl chains are unsaturated and saturated with 1,2,4 and 5 double bonds. In addition, after data evaluation we found species contributing fatty acids with an odd number of carbon atoms. As this species are produced commonly by prokaryotic cells and are not found in the eukaryotic one, they are associated with the falls positive results.

3.3 Comparison of lipid species in pig lavage and in the supernatant of amnion biopsy

Figure 25 demonstrates the distribution of lipid species which were present only in the pig lavage and in the supernatant of amnion biopsy as well as the common lipid species for both. We have found in total 43 lipid species in the pig lavage and 20 in amnion biopsy samples. These lipid species were associated into five subclasses of phospholipids: PE, PS, PC, SM, and PEO. Amongst them just five phospholipid species are found to be contained in both sample types: PE-O [16:1/20:4], PE-O [16:0/22:5], PE-O [16:1/22:4], SM [34:1] and PC [16:0/16:0].

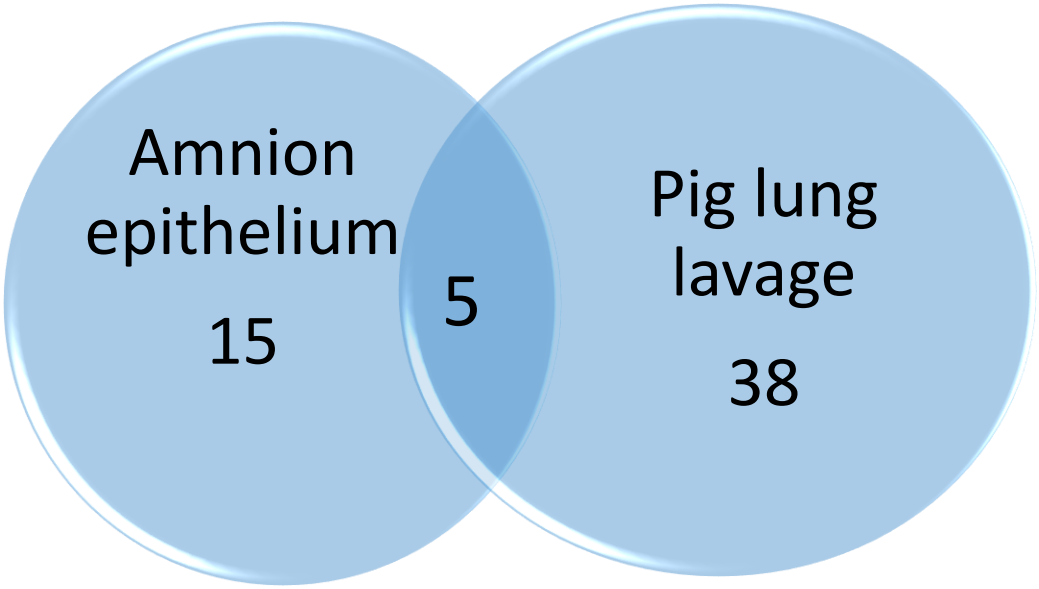

Figure 25. *The distribution of phospholipid species in the pig lavage and in the supernatant of amnion biopsy*

4. Discussion

The aim of this work was to provide information on the phospholipid profile in the pig lung lavage and in the surfactant of the amnion biopsy and to compare them. According to the preliminary studies on the LBI Trauma the amnion biopsies contained similar lipid contents as the pig lung lavage samples. Therefore, we used pig lavage as a point of reference for profile comparisons. The pig lung lavage is already investigated and is used as a DPPC source for lung treatment by preterm born infants.[2] To assess the surfactant of the amnion biopsy as a potential DPPC source firstly, conditions which influence the lipid secretion should be considered.

Two regions of the amniotic sack were investigated to determine the richest lipid profile in their surfactants. The DPPC is in the secretome of both biopsy regions contained. Thus, the amnion biopsy derived from the placental side of the amniotic sack contained generally more lipid species, than the one located on the opposite side. These lipid species were associated into five phospholipid subclasses: phosphatidylcholines (PC), phosphatidylserines (PS), sphingomyelins (SM) and phosphatidylethanolamines with ester linkage (PE) and ether linkage (PE-O). We demonstrated PE-O as the lipid richest subclass with a total sum of 171 lipids in all samples. Right after the PE-O, the PC subclass was found with 107 lipids and the SM with 101. In compression to other, the PE and the PS were lipid-poor. The lipid distribution pattern in subclasses is similar for both amnion biopsies. Hence, placental implies more phospholipids in each subclass.

Further investigations were focused on the selection of appropriate cultivation medium which will promote the lipid secretion. For this purpose, amnion biopsies were cultivated in two different media SAGM and DMEM. We found DMEM as compatible. Both biopsies showed higher lipid release after cultivation in the DMEM. The reason for such behavior is probably better preservation of the amnion biopsy in the SAGM medium. To prove such statement, additional histological images are required.

Additionally, the influence of cultivation times on the lipid profile was investigated. To announce, a general relation between the lipid species content and the cultivation time was not detected. The results showed the highest number of lipid species in samples incubated for seven days and the lowest for one incubation day. Hence, this also depends on the biopsy region and the respective subclass. The lipid content in the PD, PS and RAD was roughly dependent on the incubation time. In contrast, the content in the RAS was not time dependent.

Generally, the selection of medium type was shown as an important element for a better lipid yield regardless of the cultivation time.

In this master thesis, differences in lipid profiles between individuals were also determined. The evaluated data showed similar results for both donors. PD samples from both donors contained all common lipid species for SM, PC, PE and PS subclasses. In RAD samples, only SM and PC species were found common for both donors. The distribution of lipid species in the PS and the RAS samples is inhomogeneous. We discovered for the PE-O subclass in all amnion biopsies a non-uniform distribution as between the donors so as between samples cultivated at same incubation times in biopsy plates with different diameters. Samples in 2 cm biopsy plates are shown with more lipid species.

Tables 9, 10, 11 and 12 demonstrate similar lipid profiles in both donors which differ from the animal derived pulmonary surfactant. After lipid profile comparisons between the supernatant of the amnion biopsy and the pig lung lavage samples, five common lipid species from the SM, PC and the PE-O subclass were found. One of these common species is the DPPC. This was already expected for the pig lung lavage, due to previous reports which demonstrate the presence of DPPC in high concentrations.[63] The DPPC was also found in the supernatant of the amnion biopsy what shows potential to implement the amnion biopsy as a DPPC source. The lung lavage contains also other PC species which are not present in the amnion surfactant. Hence, they are in general contained in animal derived pulmonary surfactants,[62] such as the PC (16:0/14:0), PC (18:0/18:2), PC (16:0/20:4) and PC (18:1/18:1). The DPPC is important for the proper lung function[2,3,4] so as phosphatidylcholines which contain saturated myristic acid (14:0), palmitic acid (16:0) and the unsaturated palmitoleic acid (16:1).[62] We have found in the pig lung lavage two PC species which correspond to PC (14:0/16:0) and PC (16:1/16:1). The PC (16:0/14:0) is an important component in the lung lavage for proper lung function. In the inhalation process, it is found enriched during the alveoli development in rats.[64] The function of the PE-O and SM species in the pulmonary surfactant is less clear. In general, it is known that cholesterol and unsaturated phospholipids cause high surfactant fluidity at body temperature and therefore contribute to the faster DPPC transport from type II cells to the air/liquid interface.[4]

The total lipid profile in the pig lung lavage and the surfactant of amnion biopsy varied significantly. We were able to conclude that the highest influence on the lipid profile has the individual on its self, due to the functional conditions of the particular person or animal. This could be the reason why just five species were commonly shared by the amnion and the pig lung lavage.

Quantitative assessments of lipids in both amniotic supernatant and lung lavages were not possible by our shotgun lipidomics platform. Therefore, the determination of variation coefficients could not be achieved in a meaningful way. This makes the application of a quantitative analysis platform indispensable for further studies by combining a separation method like SFC with mass spectrometric detection.

Finally, the diversity of secreted lipids can be modulated by the selection of the cultivation medium and the biopsy position in the amniotic sack. Further, placenta associated amnion biopsy with DMEM cultivation medium is showed to stimulate the lipid release the most. Amnion is demonstrated as a potential DPPC source, but cannot yet completely replace the animal derived pulmonary surfactant, due to the lack of two more main lipid species essential for proper lung function, such as PC (16:0/14:0) and PC (16:0/16:1).[62,64]

5. Conclusion

Shotgun lipidomics is demonstrated as a suitable approach to performing qualitative lipid profiling analysis. Our results showed a large number of lipids being released from amnion biopsy derived from the placental part of the human amniotic sack, after in vitro cultivation in the DMEM medium. The lipid profile in the SAGM medium was also investigated but with fewer lipid species compared to DMEM. Additionally, the cultivation time showed for both cultivation media a slight impact on the lipid content. The amnion biopsy located on the opposite side of placenta indicated a very poor lipid profile. We demonstrated also the presence of the DPPC in the lipid secretome of both biopsy sections and in both cultivation media. This is a good sign to use it as a DPPC source. Contrarily just five common lipid species between the pig lavage and the surfactant of the amnion biopsy were observed. From a qualitative point of view, the amniotic supernatant is therefore quite different to the pig lung lavage. According to the presence of DPPC in amnion, it shows a potential as a DPPC source. In contrary PC [14:0 / 16:0] and PC [16:1 / 16:1] found in the pig lung lavage is not present in the amnion supernatant and is therefore not suitable to completely replace the pig lung lavage

The applied shotgun lipidomics analysis platform was not suitable for the assessment of quantitative information. Hence, further quantitative methods are necessary. For better understanding, a profound analysis with the biological focus would be required to determine the impact of the cultivation medium on the lipid profile.

Appendix

Chemicals, standards and instruments

Company	Product
Chemicals	
Sigma-Aldrich Laborchemikalien GmbH, St. Louis, Missouri, USA	**Tert-Butyl methyl ether (MTBE)** **Chloroform** (CHROMASOLV® Plus, for HPLC, ≥99.9%, contains amylenes as stabilizer)
VWR Chemicals, Pennsylvania, USA	**Acetonitrile** (Acetonitrile HiPerSolv CHROMANORM® ACS, Reag. Ph. Eur., super gradient grade for HPLC) **Methanol** (Methanol HiPerSolv CHROMANORM® for LC-MS)
Carl Roth GmbH + Co. KG, Karlsruhe, Germany	**2-Propanol** (ROTISOLV® HPLC)
Fluka St. Louis, Missouri, USA	**Ammonium acetate** (LC-MS Ultra) **Formic acid** (for mass spectrometry ~ 98%) **Water** (LC-MS Ultra CHROMASOLV®, tested for UHPLC-MS)
Standards	
Avanti Polar Lipids Inc., Alabama, USA	Phosphatidylcholine **PC (17:0/17:0)** Lysophosphatidylcholine **LPC (12:0)** Phosphatidylserine **PS (17:0/17:0)** Lysophosphatidylethanolamine **LPE (14:0)** Lysophosphatidylglycerol **LPG (17:0)** [Phosphatidylcholine **DPPC (16:0/16:0)** Phosphatidylcholine **PC (18:1/18:1)** Phosphatidylethanolamine **PE (18:1/18:1)** Phosphatidylserine **PS (18:1/18:0)**
Thermo Fisher Scientific, Massachusetts, USA	**Pierce™ ESI Negative** Ion Calibration Solution **Pierce™ ESI Positive** Ion Calibration Solution
Instruments	
GeneVac, Ipswich, Suffolk, UK	miVac quattro centrifugal evaporator
Bandelin SONOREX™ Digital 10 P, Berlin, Germany	Ultrasonic bath
Eppendorf, Wesseling-Berzdorf, Germany	Microcentrifuge 5424
Denver instrument, New York, USA	Balance
Eppendorf, Wesseling-Berzdorf, Deutschland	Thermomixer comfort
Scientific Industries inc., New York, USA	Vortex mixer
Advion, New York, USA	TriVersa NanoMate®
Thermo scientific, Massachusetts, USA	LTQ-Velos

Reference

[1] Schwudke, Dominik, *et al*. "Shotgun lipidomics on high resolution mass spectrometers." Cold Spring Harbor perspectives in biology 3.9 (2011): a004614.

[2] Goerke, Jon. "Pulmonary surfactant: functions and molecular composition."*Biochimica et Biophysica Acta (BBA)-Molecular Basis of Disease* 1408.2 (1998): 79-89.

[3] Veldhuizen, Edwin JA, *et al*. "The role of surfactant proteins in DPPC enrichment of surface films." Biophysical journal 79.6 (2000): 3164-3171.

[4] Perez-Gil, Jesús, and Timothy E. Weaver. "Pulmonary surfactant pathophysiology: current models and open questions." Physiology 25.3 (2010): 132-141.

[5] Modena, Alberto Bacchi, and Stefania Fieni. "Amniotic fluid dynamics." *Acta bio-medica: Atenei Parmensis* 75 (2003): 11-13.

[6] Bloomfield FH, van Zijl PL, Bauer MK & Harding JE. Effects of intrauterine growth restriction and intraamniotic insulin-like growth factor I treatment on blood and amniotic fluid concentrations and on fetal gut uptake of amino acid in late gestation ovine fetuses. J Pediatr Gastroenterol Nutr 2002; 35: 287−297.

[7] Underwood, Mark A., William M. Gilbert, and Michael P. Sherman. "Amniotic fluid: not just fetal urine anymore." Journal of Perinatology 25.5 (2005): 341-348.

[8] *http://medicine.academic.ru/363/Amnion*

[9] Willson, Douglas F., Patricia R. Chess, and Robert H. Notter. "Surfactant for pediatric acute lung injury." Pediatric Clinics of North America 55.3 (2008): 545-575.

[10] Vosdoganes, Patricia, *et al*. "Human amnion epithelial cells repair established lung injury." *Cell transplantation* 22.8 (2013): 1337-1349.

[11] Nkadi, Paul O., T. Allen Merritt, and De-Ann M. Pillers. "An overview of pulmonary surfactant in the neonate: genetics, metabolism, and the role of surfactant in health and disease." *Molecular genetics and metabolism* 97.2 (2009): 95-101.

[12] Cockshutt, Amanda M., Darryl R. Absolom, and Fred Possmayer. "The role of palmitic acid in pulmonary surfactant: enhancement of surface activity and prevention of inhibition by blood proteins." Biochimica et Biophysica Acta (BBA)-Lipids and Lipid Metabolism 1085.2 (1991): 248-256.

[13] Krill, Steven L., and Shanker L. Gupta. "Effect of a bovine lung surfactant protein isolate (SP-B/C) on Egg phosphatidylglycerol acyl chain order in a lipid mixture with dipalmitoylphosphatidylcholine and palmitic acid." Journal of pharmaceutical sciences 83.4 (1994): 539-541.

[14] Danhaive, Olivier, *et al*. "Surface film formation in vitro by infant and therapeutic surfactants: role of surfactant protein B." Pediatric research 77.2 (2014): 340-346.

[15] Murphy, Sean, *et al*. "Amnion epithelial cell isolation and characterization for clinical use." *Current protocols in stem cell biology* (2010): 1E-6.

[16] McDonald, Courtney A., *et al*. "Maintenance of human amnion epithelial cell phenotype in pulmonary surfactant." Stem cell research & therapy 5.5 (2014): 107.

[17] Vosdoganes, Patricia, *et al*. "Human amnion epithelial cells modulate hyperoxia-induced neonatal lung injury in mice." Cytotherapy 15.8 (2013): 1021-1029.

[18] Moodley, Yuben, *et al*. "Anti-inflammatory effects of adult stem cells in sustained lung injury: a comparative study." PLoS One 8.8 (2013): e69299.

[19] Kishimoto, Keiko, *et al*. "Nondestructive quantification of neutral lipids by thin-layer chromatography and laser-fluorescent scanning: suitable methods for “lipidome” analysis." Biochemical and biophysical research communications 281.3 (2001): 657-662

[20] Holčapek, Michal. "Lipidomics." Analytical and bioanalytical chemistry 407.17 (2015): 4971-4972.

[21] Fahy, Eoin, *et al*. "A comprehensive classification system for lipids." Journal of lipid research 46.5 (2005): 839-862.

[22] Ghim, Jaewang, *et al*. "Accumulating insights into the role of phospholipase D2 in human diseases." Advances in biological regulation (2015).

[23] Morrison, J. C., et al. "The lecithin/sphingomyelin ratio in cases associated with fetomaternal disease." American journal of obstetrics and gynecology 127.4 (1977): 363-368.

[24] Bradshaw, M. J., V. Brimmell, and E. P. Raynes. "PRELIMINARY COMMUNICATIONS A novel alignment technique for ferroelectric smectics." Liquid Crystals 2.1 (1987): 107-110.

[25] Vance, Jean E. "Thematic Review Series: Glycerolipids. Phosphatidylserine and phosphatidylethanolamine in mammalian cells: two metabolically related aminophospholipids." Journal of lipid research 49.7 (2008): 1377-1387.

[26] Sturbois-Balcerzak, Bénédicte, *et al*. "Structure and expression of the murine phosphatidylserine synthase-1 gene." Journal of Biological Chemistry 276.11 (2001): 8205-8212.

[27] Fadok, Valerie A., *et al*. "Loss of phospholipid asymmetry and surface exposure of phosphatidylserine is required for phagocytosis of apoptotic cells by macrophages and fibroblasts." Journal of Biological Chemistry 276.2 (2001): 1071-1077.

[28] Cantley, Lewis C. "The phosphoinositide 3-kinase pathway." Science 296.5573 (2002): 1655-1657.

[29] Goto, Takayuki, *et al*. "The expression profile of phosphatidylinositol in high spatial resolution imaging mass spectrometry as a potential biomarker for prostate cancer." PloS one 9.2 (2014): e90242.

[30] Hagio, Miki, *et al*. "Phosphatidylglycerol is essential for the development of thylakoid membranes in Arabidopsis thaliana." Plant and cell physiology 43.12 (2002): 1456-1464.

[31] Kogon, D. P., *et al*. "Amniotic fluid phosphatidylglycerol and phosphatidylcholine phosphorus as predictors of fetal lung maturity." American journal of obstetrics and gynecology 154.2 (1986): 226-230.

[32] Pulfer, Melissa, and Robert C. Murphy. "Electrospray mass spectrometry of phospholipids." *Mass spectrometry reviews* 22.5 (2003): 332-364.

[33] Kerwin, James L., Amy R. Tuininga, and L. H. Ericsson. "Identification of molecular species of glycerophospholipids and sphingomyelin using electrospray mass spectrometry." Journal of lipid research 35.6 (1994): 1102-1114.

[34] Hsu, Fong-Fu, and J. Turk. "Charge-driven fragmentation processes in diacyl glycerophosphatidic acids upon low-energy collisional activation. A mechanistic proposal." Journal of the American Society for Mass Spectrometry 11.9 (2000): 797-803.

[35] Bligh, E. Graham, and W. Justin Dyer. "A rapid method of total lipid extraction and purification." Canadian journal of biochemistry and physiology 37.8 (1959): 911-917.

[36] Folch, Jordi, M_ Lees, and G. H. Sloane-Stanley. "A simple method for the isolation and purification of total lipids from animal tissues." J Biol chem 226.1 (1957): 497-509.

[37] Bloor, Walter R. "A method for the determination of fat in small amounts of blood." Journal of Biological Chemistry 17.3 (1914): 377-384.

[38] Boyd, Eldon M. "The extraction of lipids from the red blood cells." Journal of Biological Chemistry 115.1 (1936): 37-45.

[39] Baümler, Erica R., Guillermo H. Crapiste, and Amalia A. Carelli. "Solvent extraction: kinetic study of major and minor compounds." Journal of the American Oil Chemists' Society 87.12 (2010): 1489-1495.

[40] Matyash, Vitali, *et al*. "Lipid extraction by methyl-tert-butyl ether for high-throughput lipidomics." Journal of lipid research 49.5 (2008): 1137-1146.

[41] Abbott, Sarah K., *et al*. "An improved high-throughput lipid extraction method for the analysis of human brain lipids." Lipids 48.3 (2013): 307-318.

[42] Ekroos, Kim. “Lipidomics: Technologies and Applications, Wiley-vch Verlag GmbH & Co. KGaA” (2012)

[43] Han, Xianlin, and Richard W. Gross. "Electrospray ionization mass spectroscopic analysis of human erythrocyte plasma membrane phospholipids." *Proceedings of the National Academy of Sciences* 91.22 (1994): 10635-10639.

[44] Taguchi, Ryo, *et al*. "Focused lipidomics by tandem mass spectrometry." Journal of Chromatography B 823.1 (2005): 26-36.

[45] Brügger, Britta, et al. "Quantitative analysis of biological membrane lipids at the low picomole level by nano-electrospray ionization tandem mass spectrometry." Proceedings of the National Academy of Sciences 94.6 (1997): 2339-2344.

[46] Zhang, Tingting, *et al*. "Development of a mass-spectrometry-based lipidomics platform for the profiling of phospholipids and sphingolipids in brain tissues." Analytical and bioanalytical chemistry 407.21 (2015): 6543-6555.

[47] Wang, Yan, et al. "Comprehensive ultra-performance liquid chromatographic separation and mass spectrometric analysis of eicosanoid metabolites in human samples." *Journal of Chromatography A* 1359 (2014): 60-69.

[48] Olsen, Jesper V., *et al*. "Parts per million mass accuracy on an Orbitrap mass spectrometer via lock mass injection into a C-trap." Molecular & Cellular Proteomics 4.12 (2005): 2010-2021.

[49] Han, Xianlin, Kui Yang, and Richard W. Gross. "Multi-dimensional mass spectrometry-based shotgun lipidomics and novel strategies for lipidomic analyses." Mass spectrometry reviews 31.1 (2012): 134-178.

[50] Simons, Brigitte, *et al*. "Molecular Characterization and Quantitation of Lipids with High Resolution Accurate Mass Tandem MS Techniques." AB SCIEX, Framingham, MA (2011).

[51] Advion TriVersa^{TM} NanoMate, TriVersa Uder Training, 2009

[52] Schuhmann, Kai, *et al*. "Shotgun lipidomics on a LTQ Orbitrap mass spectrometer by successive switching between acquisition polarity modes."*Journal of Mass Spectrometry* 47.1 (2012): 96-104.

[53] Graessler, Juergen, *et al*. "Top-down lipidomics reveals ether lipid deficiency in blood plasma of hypertensive patients." PloS one 4.7 (2009): e6261.

[54] LTQ Series Hardware manual, 2009

[55] Kim, Min-Sik, and Akhilesh Pandey. "Electron transfer dissociation mass spectrometry in proteomics." Proteomics 12.4-5 (2012): 530-542.

[56] Syka, John EP, et al. "Peptide and protein sequence analysis by electron transfer dissociation mass spectrometry." *Proceedings of the National Academy of Sciences of the United States of America* 101.26 (2004): 9528-9533.

[57] Herzog, Ronny, *et al*. "LipidXplorer: a software for consensual cross-platform lipidomics." PLoS One 7.1 (2012): e29851

[58] Husen, Peter, *et al*. "Analysis of lipid experiments (ALEX): a software framework for analysis of high-resolution shotgun lipidomics data." PloS one 8.11 (2013): e79736.

[59] Herzog, Ronny, *et al*. "A novel informatics concept for high-throughput shotgun lipidomics based on the molecular fragmentation query language." Genome Biol 12.1 (2011): R8.

[60] Penkov, Sider, *et al*. "Maradolipids: diacyltrehalose glycolipids specific to dauer larva in Caenorhabditis elegans." Angewandte Chemie International Edition 49.49 (2010): 9430-9435.

[61] Qian, Xiang, *et al*. "Improving the current stability through the bubbles-free microfluidic electro-spray ionizing chip." *Key Engineering Materials*. Vol. 609. 2014.

[62] Bernhard, Wolfgang, et al. "Developmental changes in rat surfactant lipidomics in the context of species variability." Pediatric pulmonology 42.9 (2007): 794-804.

[63] Bernhard, Wolfgang, *et al*. "Conductive airway surfactant: surface-tension function, biochemical composition, and possible alveolar origin." American journal of respiratory cell and molecular biology 17.1 (1997): 41-50

[64] Bernhard, Wolfgang, et al. "Developmental changes in rat surfactant lipidomics in the context of species variability." Pediatric pulmonology 42.9 (2007): 794-804.